DESIGN AND IMPLEMENTATION OF CONTROL ALGORITHMS FOR STABILIZATION OF ROTARY INVERTED PENDULUM

FATMA NUR ŞEN

JUNE 2019

DESIGN AND IMPLEMENTATION OF CONTROL ALGORITHMS FOR STABILIZATION OF ROTARY INVERTED PENDULUM

A THESIS SUBMITTED TO
THE GRADUATE SCHOOL OF NATURAL AND APPLIED
SCIENCES OF
ÇANKAYA UNIVERSITY

BY
FATMA NUR ŞEN

IN PARTIAL FULFILLMENT OF THE REQUIREMENTS FOR THE
DEGREE OF
MASTER OF SCIENCE
IN
MECHATRONICS ENGINEERING
DEPARTMENT

JUNE 2019

Title of the Thesis: **Design and Implementation of Control Algorithms for Stabilization for Rotary Inverted Pendulum**

Submitted By **Fatma Nur ŞEN**

Approval of the Graduate School of Natural and Applied Sciences, Çankaya University.

Prof. Dr. Can ÇOĞUN
Director

I certify that this thesis satisfies all the requirements as a thesis for the degree of Master of Science.

Assist. Prof. Dr. Ulaş BELDEK
Head of Department

This is to certify that we have read this thesis and that in our opinion it is fully adequate, in scope and quality, as a thesis for the degree of Master of Science.

Assist. Prof. Dr. Ulaş BELDEK
Supervisor

Examination Date: 21.06.2019

Examining Committee Members

Assist. Prof. Dr. Ali Emre TURGUT	METU	
Assist. Prof. Dr. Halit ERGEZER	Çankaya Univ.	
Assist. Prof. Dr. Ulaş BELDEK	Çankaya Univ.	

STATEMENT OF NON-PLAGIARISM PAGE

I hereby declare that all information in this document has been obtained and presented in accordance with academic rules and ethical conduct. I also declare that, as required by these rules and conduct, I have fully cited and referenced all material and results that are not original to this work.

Name, Last Name: Fatma Nur ŞEN

Signature: 

Date: 01.07.2019

ABSTRACT

DESIGN AND IMPLEMENTATION OF CONTROL ALGORITHMS FOR STABILIZATION OF ROTARY INVERTED PENDULUM

ŞEN, Fatma Nur

M.Sc., Department of Mechatronics Engineering

Supervisor: Assist. Prof. Dr. Ulaş BELDEK

JUNE 2019, 82 pages

Rotary Inverted Pendulum is a popular test-bed in control theory applications as it has a nonlinear characteristics and unstable structure. To drive the pendulum to upright position and holding the stick of the pendulum stabilized in that condition is one of the important benchmark problems in control theory. Generally, the control structure of this system consists of two modes. The first mode is known as the swing up mode where the pendulum is brought into nearly upright position from a stand still downward orientation. The second control mode is called as hold mode and it switches the swing up mode when the pendulum is in an epsilon neighborhood of the upright position and its aim is to stabilize the pendulum and keeping it motionless at this condition. The intention in this thesis is developing hold mode control structures integrating the State Feedback Control, Routh Hurwitz method and Genetic Algorithms.

Keywords: Rotary Inverted Pendulum, Genetic Algorithm, State Feedback, Routh Hurwitz, Multi Criteria Optimization.

ÖZ

DÖNER TERS SARKAÇ SİSTEMİNİN STABİLİZASYONU İÇİN KONTROL ALGORİTMALARININ TASARIMI VE UYGULANMASI

ŞEN, Fatma Nur
Yüksek Lisans, Mekatronik Mühendisliği Anabilim Dalı
Tez Yöneticisi: Dr. Öğr. Üyesi Ulaş BELDEK

HAZİRAN 2019, 82 sayfa

Döner ters sarkaç sistemi kontrol teorisi uygulamalarında popüler bir test ortamıdır. Çünkü döner ters sarkaç doğrusal olmayan özelliklere ve dengesiz bir yapıya sahiptir. Sarkacı dik pozisyona getirmek ve sarkacın çubuğunu bu durumda kararlı tutmak kontrol teorisindeki en önemli değerlendirme problemlerindendir. Genellikle, bu sistemin kontrol yapısı iki moddan oluşur. İlk mod, sarkacın hareketsiz baş aşağı pozisyondan neredeyse dik pozisyona getirildiği salınım yaparak yukarı kaldırma modu olarak bilinir. İkinci kontrol moduna tutma modu denir ve sarkaç dik pozisyonun çalışma noktası komşuluğunda olduğunda salınım yaparak yukarı kaldırma modunun yerine görevi devralır. Bunun amacı sarkacı kararlı hale getirmek ve bu durumda hareketsiz kalmasını sağlamaktır. Bu tezin amacı durum geri beslemesi kontrolü, Routh Hurwitz metodu ve Genetik Algoritmaları entegre ederek tutma modu kontrol yapılarını geliştirmektir.

Anahtar Kelimeler: Döner Ters Sarkaç Sistemi, Genetik Algoritma, Durum Geri Beslemesi, Routh Hurwitz, Çok Kriterli Optimizasyon

ACKNOWLEDGEMENTS

I would like to take this chance to acknowledge who have mentored, helped and supported me along this period.

Foremost, I would like to thank my thesis supervisor Assistant Professor Ulaş Beldek for his guidance, support and encouragement throughout this research. Your support and encouragement provided me great learning opportunities. I am grateful for your mentorship.

I would like thank my colleagues for their helped, support. Their feedback about the research are significant to augment the quality of research.

I would also like thank my parents and my brother for their support throughout my higher education journey and their support is helping me to overcome the problems in really difficult times.

Finally, I would like thank my friends for their helped and support. It is a pleasure to express my special thanks to Dilara İçkecan for her valuable support in this journey.

TABLE OF CONTENTS

LIST OF FIGURES

LIST OF TABLES

LIST OF ABBREVIATIONS

RIP	Rotary Inverted Pendulum
GA	Genetic Algorithm
Hz	Hertz
DC	Direct Current

CHAPTER 1

INTRODUCTION

1.1. Background

The inverted pendulum [1]is a well-known problem in control theory and is used to test the control strategies. Due to complex behaviors, lots of versions of inverted pendulum are developed. The rotary inverted pendulum is one of the versions of the inverted pendulum. It has also similar characteristic with inverted pendulum such as nonlinearity and instability. In real time applications, the rotary inverted pendulum is used in different areas such as transportation vehicles, rockets and missile systems and aircraft landing systems. [2]

The rotary inverted pendulum is a clear example for a system with two degrees of freedom. The working principle of this system is as follows: the pendulum is connected the horizontal arm and the arm is linked with the servo motor. The degrees of freedom of the system comes from the rotation of the horizontal arm and the motion of the inverted pendulum which are perpendicular to each other. [3]

The rotary inverted pendulum is called as Furuta [4] pendulum because rotary inverted pendulum is invented at the Tokyo Institute of Technology by Katsuhisa Furuta, a Japanese researcher, who was a pioneer for many researchers about designing control theories about the rotary inverted pendulum. Therefore, rotary inverted pendulum is a popular test-bed in control theory applications as it has a nonlinear characteristics and unstable structure. To drive the pendulum to upright position and holding the stick of the pendulum stabilized in that condition is one of the important benchmark problems in control theory.

Generally, the control structure of this system consists of two modes. The first mode is known as the swing up mode where the pendulum is brought into nearly upright position from a stand still downward position.

The second control mode is called as hold mode and it switches the swing up mode when the pendulum is in an epsilon neighborhood of the upright position and its aim is to stabilize the pendulum and keeping it motionless (nearly motionless) at this condition.

1.2. Methodology and literature survey

In order to design control strategies for rotary inverted pendulum, various methods are augmented and applied. Linear techniques such as state feedback, pole placement, and linear quadratic regulator are well known. On the other hand, nonlinear techniques such as energy based control and robust control are developed. Besides, artificial intelligence methods are also applied to develop controllers for rotary inverted pendulum. Mainly fuzzy logic and genetic algorithms can be accounted in this field. [2]

The genetic algorithm(GA)[5] is a search and optimization technique using criteria of genetics and natural selection. Genetic algorithm was evolved by John Holland in 1975 at the University of Michigan and this theorem was popularized by, one of the students of John Holland, David Goldberg.[6] Goldberg used this method to solve the problem like as controlling of gas-pipeline transmission.

GAs are also defined as simulations of the methods used when biological systems modify to their environment furnished in computer software models for solving optimization. Search techniques are used for solving problems such as in engineering, science, finance and economics. Especially, in engineering, genetic algorithm gain favor from various fields as a robust optimization tool and genetic algorithms are used in machine learning, image processing, pattern recognition and operational research.[7]

1.3. Thesis objective

The intention in this thesis is developing hold mode control structures integrating the State Feedback Control, Routh Hurwitz [8] method and Genetic Algorithms: Firstly, the linearized system dynamic model when the pendulum is in upright position is utilized in order to obtain the Routh Hurwitz array.

Then the stability criteria coming from the Routh Hurwitz array and some extra criteria coming from the system's closed loop poles' relative locations due to state feedback and an extra criterion coming from the restriction of gain values at the state feedback control process are integrated into the cost function of the genetic algorithm search that yields a suitable state feedback gain values. Hence the genetic algorithm search represents a multi criteria cost optimization process and depending on different choices of parameters in contribution of the cost function, the search has given interesting and promising results.

1.4. Organization of thesis

The organization of the remaining part of the thesis is as follows; in Chapter 2 the system description, the mathematical model of the rotary inverted pendulum and the linearization procedure of this system is explained. In Chapter 3, the controller design strategies, state feedback controller and genetic algorithms, and Routh Hurwitz stability criterion are mentioned briefly. In Chapter 4, the simulation and experimental results are both tabulated and shown graphically. Lastly, in Chapter 5, all work done in this thesis are summarized and it clarify the outcomes of this thesis and the future works briefly.

CHAPTER 2

SYSTEM DESCRIPTION

2.1 System description

The Quanser rotary inverted pendulum (ROTPEN) is illustrated in Figure 2.1. [9] The rotary inverted pendulum is made up of three major parts: a motor, a rotary arm and pendulum. A DC voltage is applied to the motor and by this way it supplies the necessary actuating motion signals to the arm. The motor is attached to the load gear. This gear is used to reduce the speed and transmit the motion to the arm. In this ROTPEN, the motor is classified as a servo motor SRV02. SRV02 is suitable for obtaining faster response compared to traditional DC motors as it has low inductance and rotor inductance values as well as a high efficiency value. In addition, three sensors are fitted. These sensors are tachometer, encoder and potentiometer. The encoder and potentiometer is used the measure the angular positon of the load gear and the tachometer is used for the velocity of the motor.

In one end the rotary arm it is attached to the load gear via pin and from the other end it is connected the metal shaft. This rotary arm is actuated by the motor and it rotates on a horizontal plane. The pendulum stick is connected the shaft via a T-fitting and it has a perpendicular motion with respect to the motion of the rotary arm. The pendulum rotates 360° freely on the vertical plane. Furthermore, the determine the angular position of the pendulum, another encoder is also used that is connected to the shaft.

The rotary inverted pendulum system can be represented as a Single Input Multiple Output (SIMO) system where the input is the applied DC motor voltage and the system states and outputs can be assigned as the arm angle ($x_1 = \theta$), inverted pendulum angle ($x_2 = \alpha$) and angular velocities of the arm and the inverted pendulum ($x_3 = \dot{\theta}, x_4 = \dot{\alpha}$)

As the system structure is inspected, it is observed that the set of unstable equilibrium points are reached when the pendulum is at upright position ($\alpha = 0°$) with any arm angle value and the stable equilibrium points are reached when the pendulum is at downright position ($\alpha = 180°$) with any arm angle value (reached when all the states derivatives are equal to 0).

The mission of balancing the inverted pendulum in vertical position, at one of the unstable equilibrium points starting from one of the stable equilibrium points is called as Swing Up and Hold (Stabilization) process. In this thesis, hold (stabilization) position is focused. Hence, set of equilibrium points are defined in upright position when the pendulum angle equals to zero $\alpha = 0)$.

Figure 2.1: *SRV02 ROTPEN system*

2.2 System components

The components of ROTPEN are described in Table 2.1 and associated locations of these components are given in Figure 2.2. [10]

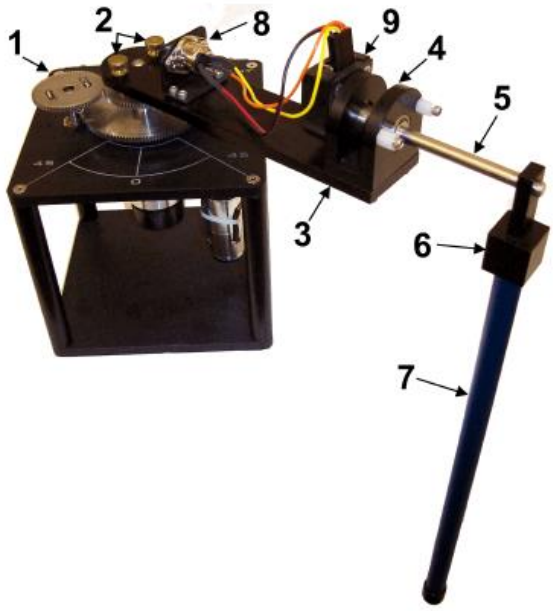

Figure 2.2: *The components of ROTPEN*

Table 2.1: *The ROTPEN components*

ID	Components	ID	Components
1	SRV02	6	Pendulum T Fitting
2	Thumbscrews	7	Pendulum Link
3	Rotary Arm	8	Pendulum Encoder Connector
4	Shaft Housing	9	Pendulum Encoder
5	Shaft		

2.3 System dynamics

The rotary inverted pendulum diagram is represented in Figure 2.3.[11]

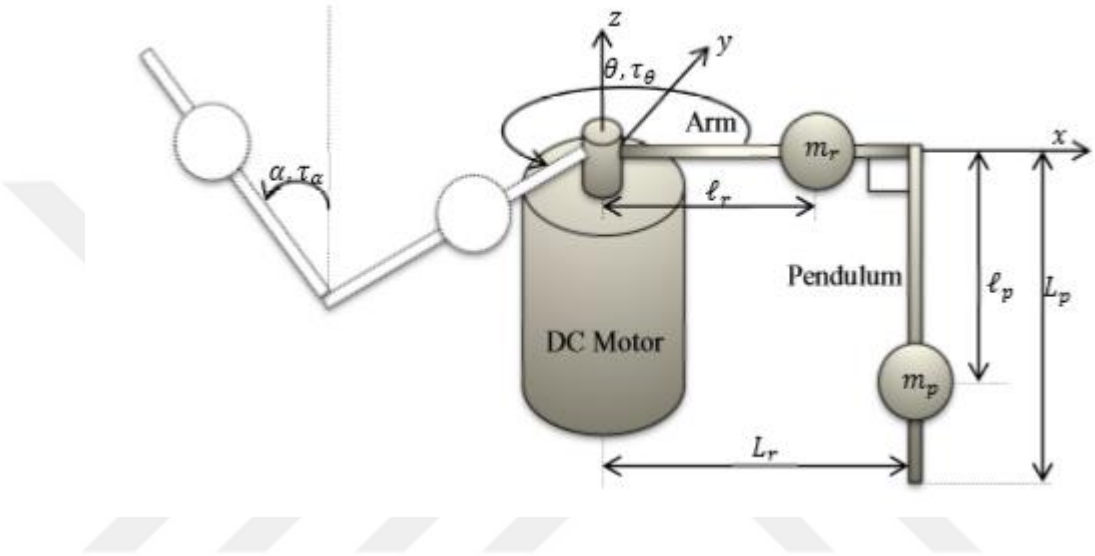

Figure 2.3: *The rotary inverted pendulum diagram*

According to the diagram, the Cartesian coordinate system is used to determine the location of the arm and the pendulum. X axis is horizontal, vertical side is z axis and finally y axis is determined accordingly. Origin of the system is assumed as a center of the arm's pivot. L_p, ℓ_p and α are total length of pendulum, the pendulum length from the arm's pivot to center of mass of pendulum and the angle of the pendulum respectively. The angle of pendulum is positive when the pendulum is rotated counterclockwise in the plane perpendicular to the arm. θ is the rotation angle of the arm with respect around z axis. L_r and ℓ_r are the total length of the arm and the length from the pivot to the center of mass of the arm respectively. Finally, $\boldsymbol{\tau_\alpha}$ is the torque which affected the pendulum due to the viscous friction and $\boldsymbol{\tau_\theta}$ is the torqued that applied to the arm.

The dynamic equations of rotary inverted pendulum depend on the center of mass of the arm and the pendulum.

In order to find the center of masses, the position of the pendulum and the arm is found. From Figure 2.4 and 2.5[11] top and front views of the system are used.

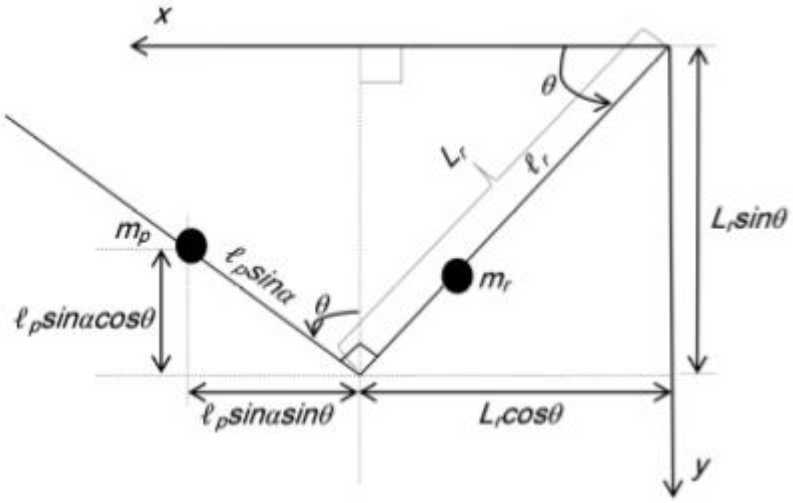

Figure 2.4: *The top view of rotary inverted pendulum*

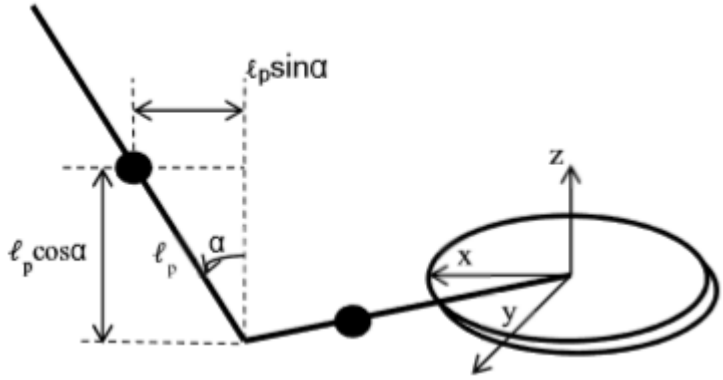

Figure 2.5: *The front view of rotary inverted pendulum*

The position of the center of mass of the pendulum are given by the following x, y and z coordinate values:

$$x_p = L_r \cos\theta + \ell_p \sin\alpha \sin\theta \tag{2.1}$$

$$y_p = L_r \sin\theta - \ell_p \sin\alpha \cos\theta \tag{2.2}$$

$$z_p = \ell_p \cos\alpha \tag{2.3}$$

The position of the center of mass of the arm are given by the following x, y and z coordinate values:

$$x_r = \ell_r \cos\theta \tag{2.4}$$

$$y_r = \ell_r \sin\theta \tag{2.5}$$

$$z_r = 0 \tag{2.6}$$

The velocity of the pendulum and arm is necessary to calculate the kinetic energy of the system. Hence, the position of pendulum and arm are differentiated with respect to time. V_p ($V_{p,x}$, $V_{p,y}$, $V_{p,z}$) and V_r ($V_{r,x}$,$V_{r,y}$, $V_{r,z}$) denote the velocity components of pendulum and arm respectively.

$$V_{p,x} = -L_r\dot{\theta}\sin\theta + \ell_p\dot{\alpha}\cos\alpha\sin\theta + \ell_p\dot{\theta}\cos\theta\sin\alpha \tag{2.7}$$

$$V_{p,y} = L_r\dot{\theta}\cos\theta - \ell_p\dot{\alpha}\cos\alpha\cos\theta + \ell_p\dot{\theta}\sin\alpha\sin\theta \tag{2.8}$$

$$V_{p,z} = -\ell_p\dot{\alpha}\sin\alpha \tag{2.9}$$

$$V_{r,x} = -\ell_r\dot{\theta}\sin\theta \tag{2.10}$$

$$V_{r,y} = \ell_r\dot{\theta}\cos\theta \tag{2.11}$$

$$V_{r,z} = 0 \tag{2.12}$$

Due to the formulation of kinetic energy, the square of the velocities of the arm and the pendulum should be calculated.

The velocity of the pendulum is

$$V_p = \sqrt{({V_{p,x}}^2 + {V_{p,y}}^2 + {V_{p,z}}^2)} \tag{2.13}$$

where

$$V_{p,x}{}^2 = L_r{}^2\dot{\theta}^2 \sin^2\theta + \ell_p{}^2\dot{\theta}^2 \sin^2\alpha \cos^2\theta + \ell_p{}^2\dot{\alpha}^2 \sin^2\theta \cos^2\alpha - 2L_r\ell_p\dot{\theta}^2 \sin\alpha \sin\theta \cos\theta - 2L_r\ell_p\dot{\alpha}\dot{\theta} \sin\alpha \sin^2\theta \cos\alpha + 2\ell_p{}^2\dot{\alpha}\dot{\theta} \sin\alpha \cos\alpha \sin\theta \cos\theta \quad (2.14)$$

$$V_{p,y}{}^2 = L_r{}^2\dot{\theta}^2 \cos^2\theta + \ell_p{}^2\dot{\theta}^2 \sin^2\alpha \sin^2\theta + \ell_p{}^2\dot{\alpha}^2 \cos^2\alpha \cos^2\theta + 2L_r\ell_p\dot{\theta}^2 \sin\alpha \sin\theta \cos\theta - 2L_r\ell_p\dot{\alpha}\dot{\theta} \sin\alpha \cos^2\theta \cos\alpha - 2\ell_p{}^2\dot{\alpha}\dot{\theta} \sin\alpha \cos\alpha \sin\theta \cos\theta \quad (2.15)$$

$$V_{p,z}{}^2 = \ell_p{}^2\dot{\alpha}^2 \sin^2\alpha \quad (2.16)$$

After some simplified steps, $V_p{}^2$ becomes,

$$V_p{}^2 = \ell_p{}^2\dot{\alpha}^2 \sin^2\alpha + L_r{}^2\dot{\theta}^2 + \ell_p{}^2\dot{\alpha}^2 - 2L_r\ell_p\dot{\alpha}\dot{\theta} \cos\alpha \quad (2.17)$$

For the arm;

$$V_r = \sqrt{V_{r,x}{}^2 + V_{r,y}{}^2 + V_{r,z}{}^2} \quad (2.18)$$

$$V_{r,x}{}^2 = \ell_r{}^2\dot{\theta}^2 \sin^2\theta \quad (2.19)$$

$$V_{r,y}{}^2 = \ell_r{}^2\dot{\theta}^2 \cos^2\theta \quad (2.20)$$

$$V_{r,z}{}^2 = 0 \quad (2.21)$$

When the components simplified, $V_r{}^2$ becomes,

$$V_r{}^2 = \ell_r{}^2\dot{\theta}^2 \quad (2.22)$$

2.4. Lagrange method

A Lagrangian formulation is used to define the equation of motions of the mechanical system and it is a common approach for robot and multiple joint systems. In Lagrange method, equations are used to transform Cartesian coordinates into the generalized coordinates (q_i).

Then, the general terms of Lagrangian formulation are

$$L\big(q(t),\dot{q}(t)\big) = K\big(q(t),\dot{q}(t)\big) - U\big(q(t)\big) \tag{2.23}$$

K represents the Kinetic Energy. Kinetic Energy can be due to rotational and translational motions and for this reason it can be written as a function of generalized coordinate variables q(t) and their derivatives $\dot{q}(t)$. U shows the Potential Energy. The potential energy is created via conservative forces such as gravity and springs. Hence this energy is related only with the generalized coordinate variables q(t). Associated with these information, Lagrange formulation is defined as;

$$L = K - U \tag{2.24}$$

The Euler-Lagrange equations for n degrees of freedom system:

$$\frac{d}{dt}\left(\frac{\partial L}{\partial \dot{q}_i}\right) - \frac{\partial L}{\partial q_i} = Q_i \tag{2.25}$$

where i=1,….,n and Q_i describes the generalized force. It is supplied from external forces. These forces should be non-conservative external forces. (e.g. friction)

The rotary inverted pendulum has two-degrees of freedom. Hence, the angles of pendulum and arm (α and θ) are generalized coordinates in this system. The first generalized coordinate is taken as the position of the arm (θ) and the second generalized coordinate is taken as the position of the pendulum (α). And the generalized forces are defined as:

$$Q_1 = \tau_\theta = \tau - B_r\dot{\theta} \tag{2.26}$$

$$Q_2 = \tau_\alpha = -B_p\dot{\alpha} \tag{2.27}$$

B_r and B_p are viscous damping coefficient. τ describes the torque applied on the arm which is generated via servo motor. Additionally

$$\tau = \frac{\eta_g k_g \eta_m k_t\left(V_m - k_g k_m \dot{\theta}\right)}{R_m} \tag{2.28}$$

Where

- η_g and η_m : the gearbox efficiency and the motor efficiency .
- k_t ,k_g and k_m : the motor-torque constant, the gear ratio and the back-emf constant
- R_m: the armature resistance
- V_m: the back – emf voltage

Then the Euler –Lagrange equations of the rotary inverted pendulum are defined as

$$\frac{d}{dt}\left(\frac{\partial L}{\partial \dot{\theta}}\right) - \frac{\partial L}{\partial \theta} = \tau - B_r\dot{\theta} \tag{2.29}$$

$$\frac{d}{dt}\left(\frac{\partial L}{\partial \dot{\alpha}}\right) - \frac{\partial L}{\partial \alpha} = -B_p\dot{\alpha} \tag{2.30}$$

The total kinetic energy of the system:

$$K_T = K_p + K_r \tag{2.31}$$

K_p and K_r are total kinetic energy of pendulum and arm respectively.

For the pendulum:

$$K_p = K_{P,translational} + K_{p,rotational} \tag{2.32}$$

$$K_{P,translational} = \frac{1}{2} m_p {v_p}^2 \tag{2.33}$$

$$K_{P,translational} = \frac{1}{2} m_p {\ell_p}^2 \dot{\alpha}^2 \sin^2\alpha + {L_r}^2\dot{\theta}^2 + {\ell_p}^2\dot{\alpha}^2 - 2L_r\ell_p\dot{\alpha}\dot{\theta}\cos\alpha \tag{2.34}$$

$$K_{P,rotational} = \frac{1}{2} J_p\dot{\alpha}^2 + \frac{1}{2} J_p \sin^2\alpha\,\dot{\theta}^2 \tag{2.35}$$

The equation (2.34) and (2.35) substituted into the equation (2.32)

$$K_p = \frac{1}{2} m_p {\ell_p}^2 \dot{\alpha}^2 \sin^2 \alpha + {L_r}^2 \dot{\theta}^2 + {\ell_p}^2 \dot{\alpha}^2 - 2 L_r \ell_p \dot{\alpha} \dot{\theta} \cos \alpha + \frac{1}{2} J_p \dot{\alpha}^2 + \frac{1}{2} J_p \sin^2 \alpha \, \dot{\theta}^2 \quad (2.36)$$

For the arm:

$$K_r = K_{r,translational} + K_{r,rotational} \quad (2.37)$$

$$K_{r,translational} = \frac{1}{2} m_r {v_r}^2 \quad (2.38)$$

$$K_{r,translational} = \frac{1}{2} m_r {\ell_r}^2 \dot{\theta}^2 \quad (2.39)$$

$$K_{r,rotational} = \frac{1}{2} J_r \dot{\theta}^2 \quad (2.40)$$

The equation (2.37) and (2.38) substituted into equation (2.35);

$$K_r = \frac{1}{2} m_r {\ell_r}^2 \dot{\theta}^2 + \frac{1}{2} J_r \dot{\theta}^2 \quad (2.41)$$

The total kinetic energy of the system;

$$K_T = \frac{1}{2} m_p {\ell_p}^2 \dot{\alpha}^2 \sin^2 \alpha + {L_r}^2 \dot{\theta}^2 + {\ell_p}^2 \dot{\alpha}^2 - 2 L_r \ell_p \dot{\alpha} \dot{\theta} \cos \alpha + \frac{1}{2} J_p \dot{\alpha}^2 + \frac{1}{2} J_p \sin^2 \alpha \, \dot{\theta}^2 + \frac{1}{2} m_r {\ell_r}^2 \dot{\theta}^2 + \frac{1}{2} J_r \dot{\theta}^2 \quad (2.42)$$

The potential energy of the rotary inverted pendulum occurs only due to the gravity and only pendulum generates the energy. So,

$$U = m_p g h \quad (2.43)$$

Where $h = (1 - \cos \alpha)$

The potential energy is in downward position. So, equation is denoted as a;

$$U = -m_p g \ell_p (1 - \cos \alpha) \quad (2.44)$$

Using Lagrange formulation (2.24), the Lagrange formulation of the rotary inverted pendulum is;

$$L = \frac{1}{2}\dot{\theta}^2\left(m_p {L_r}^2 + \sin^2\alpha\left(J_p + m_p {\ell_p}^2\right) + J_r + m_r {\ell_r}^2\right) + \frac{1}{2}\dot{\alpha}^2\left(m_p {\ell_p}^2 + J_p\right) - m_p L_r \ell_p \dot{\alpha}\dot{\theta}\cos\alpha + m_p g \ell_p (1 - \cos\alpha) \quad (2.45)$$

The components of the Euler-Lagrange equation for the first generalized coordinates;

$$\frac{\partial L}{\partial \theta} = 0 \quad (2.46)$$

$$\frac{\partial L}{\partial \dot{\theta}} = \dot{\theta}\left(m_p {L_r}^2 + \sin^2\alpha\left(J_p + m_p {\ell_p}^2\right) + J_r + m_r {\ell_r}^2\right) - m_p L_r \ell_p \dot{\alpha}\cos\alpha \quad (2.47)$$

$$\frac{d}{dt}\left(\frac{\partial L}{\partial \dot{\theta}}\right) = \ddot{\theta}\left(m_p {L_r}^2 + \sin^2\alpha\left(J_p + m_p {\ell_p}^2\right) + J_r + m_r {\ell_r}^2\right) + 2\left(J_p + m_p {\ell_p}^2\right)\dot{\alpha}\dot{\theta}\cos\alpha\sin\alpha - \ddot{\alpha}\left(m_p L_r \ell_p \cos\alpha\right) + m_p L_r \ell_p \dot{\alpha}^2 \sin\alpha \quad (2.48)$$

Substitute these components, equation (2.44) and (2.46), into equation (2.29), the first nonlinear equation becomes;

$$\ddot{\theta}\left(m_p {L_r}^2 + \sin^2\alpha\left(J_p + m_p {\ell_p}^2\right) + J_r + m_r {\ell_r}^2\right) - \ddot{\alpha}\left(m_p L_r \ell_p \cos\alpha\right) + \dot{\theta}\left(\left(J_p + m_p {\ell_p}^2\right)\dot{\alpha}\cos\alpha\sin\alpha\right) + \dot{\alpha}\left(\left(J_p + m_p {\ell_p}^2\right)\dot{\theta}\cos\alpha\sin\alpha + m_p L_r \ell_p \dot{\alpha}\sin\alpha\right) = \tau - B_r\dot{\theta} \quad (2.49)$$

When the all terms are collected, the first nonlinear equation is;

$$\ddot{\theta}\left(m_p {L_r}^2 + \sin^2\alpha\left(J_p + m_p {\ell_p}^2\right) + J_r + m_r {\ell_r}^2\right) - \ddot{\alpha}\left(m_p L_r \ell_p \cos\alpha\right) + \dot{\theta}\left(B_r + \left(J_p + m_p {\ell_p}^2\right)\dot{\alpha}\cos\alpha\sin\alpha\right) + \dot{\alpha}\left(\left(J_p + m_p {\ell_p}^2\right)\dot{\theta}\cos\alpha\sin\alpha + m_p L_r \ell_p \dot{\alpha}\sin\alpha\right) = \tau \quad (2.50)$$

For the second generalized coordinates (pendulum position), the components of the Euler – Lagrange equation are calculated as

$$\frac{\partial L}{\partial \alpha} = \left(J_p + m_p {\ell_p}^2\right)\dot{\theta}^2 \cos\alpha \sin\alpha + m_p L_r \ell_p \dot{\alpha}\dot{\theta} \sin\alpha + m_p g \ell_p \sin\alpha \tag{2.51}$$

$$\frac{\partial L}{\partial \dot{\alpha}} = \left(J_p + m_p {\ell_p}^2\right)\dot{\alpha} - m_p L_r \ell_p \dot{\theta} \cos\alpha \tag{2.52}$$

$$\frac{d}{dt}\left(\frac{\partial L}{\partial \dot{\alpha}}\right) = \ddot{\theta}\left(-m_p L_r \ell_p \cos\alpha\right) + \ddot{\alpha}\left(J_p + m_p {\ell_p}^2\right) + m_p L_r \ell_p \dot{\alpha}\dot{\theta} \sin\alpha \tag{2.53}$$

The second nonlinear equation is defined as

$$\ddot{\theta}\left(-m_p L_r \ell_p \cos\alpha\right) + \ddot{\alpha}\left(J_p + m_p {\ell_p}^2\right) + \dot{\theta}\left(-\left(J_p + m_p {\ell_p}^2\right)\dot{\theta} \sin\alpha \cos\alpha\right) - m_p g \ell_p \sin\alpha = -B_p \dot{\alpha} \tag{2.54}$$

When all terms are collected in the left hand side of the equation, the second nonlinear equation will be

$$\ddot{\theta}\left(-m_p L_r \ell_p \cos\alpha\right) + \ddot{\alpha}\left(J_p + m_p {\ell_p}^2\right) + \dot{\theta}\left(-\left(J_p + m_p {\ell_p}^2\right)\dot{\theta} \sin\alpha \cos\alpha\right) - m_p g \ell_p \sin\alpha + B_p \dot{\alpha} = 0 \tag{2.55}$$

The dynamic equations are highly non-linear. In order to find transfer functions of system and design the controller, these equations should be linearized. The equation (2.28) is substituted into nonlinear equation (2.50) for linearization.

2.5 Linearization

The common method for linearization is Taylor series expansion. Accordance with this theorem, a non-linear function f*(z)* which depends on multiple inputs or states *z* is defined where $z = (z_1, z_2, z_3 \dots\dots, z_n)$. Then, the corresponding linearized function $f_{lin}(z)$ at the operating point $z_0 = (a, b, \dots., n)$ is:

$$f_{lin}(z) = f(z_0) + \left(\frac{\partial f(z)}{\partial (z_1)}\right)|_{z=z_0}(z_1 - a) + \cdots + \left(\frac{\partial f(z)}{\partial (z_n)}\right)|_{z=z_0}(z_n - n) \tag{2.56}$$

For the rotary inverted pendulum, z variables are defined as a $z^T = [\ddot{\theta}, \ddot{\alpha}, \dot{\theta}, \dot{\alpha}, \theta, \alpha]$

And for this set up all initial conditions are zero.

Hence, equilibrium points are: ${z_0}^T = [0,0,0,0,0,0]$.

For the first non-linear equation

$$f_{lin,1}(z) = f(z_0) + \left(\frac{\partial f(z)}{\partial(\ddot{\theta})}\right)|_{z=0}(\ddot{\theta}) + \left(\frac{\partial f(z)}{\partial(\ddot{\alpha})}\right)|_{z=0}(\ddot{\alpha}) + \left(\frac{\partial f(z)}{\partial(\dot{\theta})}\right)|_{z=0}(\dot{\theta}) + \left(\frac{\partial f(z)}{\partial(\dot{\alpha})}\right)|_{z=0}(\dot{\alpha}) + \left(\frac{\partial f(z)}{\partial(\theta)}\right)|_{z=0}(\theta) + \left(\frac{\partial f(z)}{\partial(\alpha)}\right)|_{z=0}(\alpha) \quad (2.57)$$

$$\left(\frac{\partial f(z)}{\partial(\ddot{\theta})}\right)|_{z=0} = {m_p L_r}^2 + \sin^2\alpha\left(J_p + m_p {\ell_p}^2\right) + J_r + m_r {\ell_r}^2 = {m_p L_r}^2 + J_r + m_r {\ell_r}^2$$

$$\left(\frac{\partial f(z)}{\partial(\ddot{\alpha})}\right)|_{z=0} = -m_p L_r \ell_p \cos\alpha = -m_p L_r \ell_p$$

$$\left(\frac{\partial f(z)}{\partial(\dot{\theta})}\right)|_{z=0} = \left(B_r + \left(J_p + m_p {\ell_p}^2\right)\dot{\alpha}\cos\alpha\sin\alpha\right) + \frac{\eta_g k_g \eta_m k_t\left(k_g k_m\right)}{R_m}$$

$$= B_r + \frac{\eta_g k_g \eta_m k_t\left(k_g k_m\right)}{R_m}$$

The other $\dot{\alpha}, \theta, \alpha$ based derivatives are zero and $f(z_0) = 0$. The first linear equation becomes;

$$\left({m_p L_r}^2 + J_r + m_r {\ell_r}^2\right)\ddot{\theta} + \left(-m_p L_r \ell_p\right)\ddot{\alpha} + \left(B_r + \frac{\eta_g k_g \eta_m k_t\left(k_g k_m\right)}{R_m}\right)\dot{\theta} = \frac{\eta_g k_g \eta_m k_t V_m}{R_m} \quad (2.58)$$

For the other non-linear equation using equation (2.57);

$$f_{lin,2}(z) = f(z_0) + \left(\frac{\partial f(z)}{\partial(\ddot{\theta})}\right)|_{z=0}(\ddot{\theta}) + \left(\frac{\partial f(z)}{\partial(\ddot{\alpha})}\right)|_{z=0}(\ddot{\alpha}) + \left(\frac{\partial f(z)}{\partial(\dot{\theta})}\right)|_{z=0}(\dot{\theta}) + \left(\frac{\partial f(z)}{\partial(\dot{\alpha})}\right)|_{z=0}(\dot{\alpha}) + \left(\frac{\partial f(z)}{\partial(\theta)}\right)|_{z=0}(\theta) + \left(\frac{\partial f(z)}{\partial(\alpha)}\right)|_{z=0}(\alpha)$$

$$\left(\frac{\partial f(z)}{\partial(\ddot{\theta})}\right)|_{z=0} = -m_p L_r \ell_p \cos\alpha = -m_p L_r \ell_p$$

$$\left(\frac{\partial f(z)}{\partial(\ddot{\alpha})}\right)|_{z=0} = J_p + m_p {\ell_p}^2$$

$$\left(\frac{\partial f(z)}{\partial(\dot{\alpha})}\right)|_{z=0} = B_p$$

$$\left(\frac{\partial f(z)}{\partial(\alpha)}\right)|_{z=0} = -m_p g \ell_p$$

The other $\dot{\theta}, \theta$ based derivatives are zero and $f(z_0) = 0$. The second linear equation becomes:

$$\left(-m_p L_r \ell_p\right)\ddot{\theta} + \left(J_p + m_p {\ell_p}^2\right)\ddot{\alpha} - m_p g \ell_p \alpha = 0 \tag{2.59}$$

2.6 State space representation

The linear state space equations define as

$$\dot{x} = Ax + Bu \tag{2.60}$$

$$y = Cx + Du \tag{2.61}$$

Where x represents the state and u is control input. A, B, C and D define as a system, input, output and direct coupled matrices, respectively.

There are some parameters to ease the task for linear equations of the rotary inverted pendulum;

$$\beta = J_r + m_r {\ell_r}^2 + m_p {L_r}^2$$

$$\rho = J_p + m_p {\ell_p}^2$$

$$\delta = m_p L_r \ell_p$$

$$\gamma = m_p \ell_p g$$

$$J_T = J_p m_p {L_r}^2 + m_p m_r {\ell_p}^2 {\ell_r}^2 + J_r m_p {\ell_p}^2 + J_p m_r {\ell_r}^2 + J_p J_r$$

$$T_1 = \frac{\eta_g k_g \eta_m \, k_t \left(k_g k_m \dot{\theta}\right)}{R_m}$$

$$T_2 = \frac{\eta_g k_g \eta_m \, k_t (V_m)}{R_m}$$

To obtain the state space model, the states are defined as $x_1 = \theta$, $x_2 = \alpha$, $x_3 = \dot{\theta}$ and $x_4 = \dot{\alpha}$. With these states, the linear equations of rotary inverted pendulum are written in matrices form as

$$A = \begin{bmatrix} 0 & 0 & 1 & 0 \\ 0 & 0 & 0 & 1 \\ 0 & \gamma\delta/J_T & -\rho(B_r + T_1)/J_T & -\delta B_p/J_T \\ 0 & \gamma\beta/J_T & -\delta(B_r + T_1)/J_T & -\beta B_p/J_T \end{bmatrix} \tag{2.62}$$

$$B = \begin{bmatrix} 0 \\ 0 \\ (\rho T_2)/J_T \\ (\delta T_2)/J_T \end{bmatrix} \tag{2.63}$$

Only the position of the servo and link angles are measured. Hence, the output matrix becomes:

$$C = \begin{bmatrix} 1 & 0 & 0 & 0 \\ 0 & 1 & 0 & 0 \end{bmatrix} \tag{2.64}$$

$$D = \begin{bmatrix} 0 \\ 0 \end{bmatrix} \tag{2.65}$$

2.7 System parameters

The all system parameters are presented in Table 2.2 and these parameters are taken user manual of the set-up and manual of the SRV02.[12]

The parameters of the system are substituted into system and input matrices;

$$A = \begin{bmatrix} 0 & 0 & 1 & 0 \\ 0 & 0 & 0 & 1 \\ 0 & 53.29853 & -16.5724 & -0.6582 \\ 0 & 108.2996 & -19.5897 & -1.3373 \end{bmatrix} \tag{2.66}$$

$$B = \begin{bmatrix} 0 \\ 0 \\ 29.8002 \\ 35.2259 \end{bmatrix} \tag{2.67}$$

The eigenvalues of the systems are 0, -4.6674, -20.9277, 7. 6853.As it can be seen that, one of the poles of system is on the right side of the plane. Hence, the system is unstable.

Table 2.2: *The system parameters*

Symbol	Description	Value	Unit
m_p	Mass of pendulum	0.127	kg
L_p	Total length of pendulum	0.337	m
l_p	Distance from pivot to center of mass	0.156	m
J_p	Pendulum moment of inertia about center of mass	0.0012	$kg.m^2$
B_p	Pendulum viscous damping coefficient as seen at the pivot axis	0.0024	N.m.s/rad
m_r	Mass of rotary arm with two thumbscrews	0.257	kg
r	Rotary arm length from pivot to tip	0.216	m
l_r	Rotary arm length from pivot to center of mass	0.0619	m
$J_{r,cm}$	Rotary arm moment of inertia about its center of mass	$9.98\ 10^{-4}$	$kg.m^2$
m_b	Rotary arm viscous damping coefficient as seen at the pivot axis	0.0024	N.m.s/rad
J_r	Rotary arm moment of inertia about pivot	0.0020	$kg.m^2$
K_{enc}	Pendulum encoder resolution	4096	counts/rev
B_r	Viscous damping coefficient of arm	0.0024	Nms/rad
L_r	Total length of arm	0.256	m
R_m	Armature resistance	2.6	Ω
B_{eq}	Equivalent viscous damping coefficient	0.015	Nms/rad
J_{eq}	Equivalent moment of inertia	0.00358	kgm^2
k_g	SVR02 system gear ratio	70	--
k_m	Back-emf constant	7.68×10^3	Vs/rad
k_t	Motor-torque constant	7.68×10^3	Nm/A
η_g	Gearbox efficiency	0.9	---
η_m	Motor efficiency	0.69	---

CHAPTER 3

CONTROLLERS DESIGN

In this chapter, two different controller design approaches depending on state feedback control method that are applicable for hold mode of control for inverted pendulum are considered. In the first on state feedback is directly applied to the inverted pendulum via a suitable pole placement procedure. In the second one pole placement procedure is carried out using Genetic Algorithms such that the state feedback gain values are determined due to a multi criteria optimization procedure.

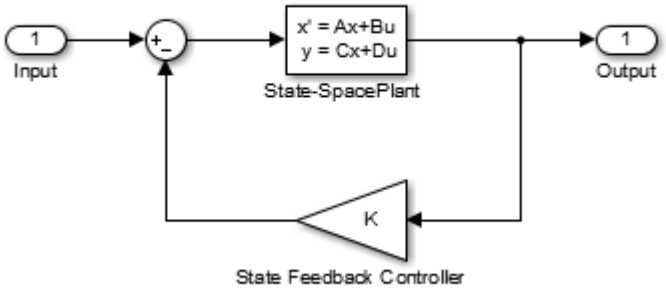

Figure 3.1: *The sample block diagram of the system*

According to the Figure 3.1, the system has a state feedback controller. Each state which is defined in chapter 2, has a proportional gain value and hence K the gain vector is defines as

$$K = [K_1 \quad K_2 \quad K_3 \quad K_4]$$

K_1 is the proportional gain of the angular position of arm (θ), K_2 is the proportional gain of angular position of the inverted pendulum (α) and K_3, K_4 are defined as proportional gain values of angular velocities of arm and inverted pendulum, respectively.

3.1 The state feedback control

The locations of closed loop poles of the system effects the transient and steady responses of the system. If the system is fully controllable, the controllability matrix has full rank and all eigenvalues can be placed at any desired locations by a suitable choice of state feedback gain. The linearized system model has the following state space representation

$$\dot{x} = Ax + Bu \tag{3.1}$$

and using state feedback the control signal can be computed using,

$$u = r(t) - Kx(t) \tag{3.2}$$

Where *K* is feedback gain, *r(t)* is reference input or desired behavior and *x(t)* is the state variable vector. When equation (3.1) is substituted into equation (3.2), one gets

$$\dot{x} = (A - BK)x + Br \tag{3.3}$$

In equation (3.3) a new system matrix is obtained due to state feedback

$$A^* = (A - BK)$$

If a system is completely controllable, it is possible to replace each eigenvalue of the system to desired locations using state feedback. The controllability of a system is checked using controllability test. According to this test, the n^{th} order linear and time invariant system is completely controllable if and only if the n×nr (r: size of input matrix) composite controllability matrix M.

$$M = [B : AB : A^2B : \ldots . : A^{n-1}B] \tag{3.4}$$

is rank of n.

If (A, B) are controllable and B *nx1* the system is represented in controllable canonical form.

The controllable canonical form;

$$\tilde{A} = \begin{bmatrix} 0 & 1 & \cdots & 0 \\ 0 & 0 & \cdots & 0 \\ \vdots & \vdots & \ddots & \vdots \\ 0 & 0 & \cdots & 1 \\ -a_1 & -a_2 & \cdots & -a_n \end{bmatrix} \tag{3.5}$$

$$\tilde{B} = \begin{bmatrix} 0 \\ 0 \\ \vdots \\ 1 \end{bmatrix} \tag{3.6}$$

If these matrices are not in controllable canonical form, there is a linear transformation P which brings them into controllable canonical form.

$$P = M\widetilde{M}^{-1} \tag{3.7}$$

Where $\widetilde{M} = \left[\tilde{B} \vdots \tilde{B}\tilde{A} \vdots \cdots \vdots \tilde{B}\tilde{A}^n\right]$ (3.8)

$$P^{-1}AP = \tilde{A} \tag{3.9}$$

$$P^{-1}B = \tilde{B} \tag{3.10}$$

Using these new matrices, the gain $\widetilde{K}$ is calculated via desired locations. For the finding original feedback gain;

$$K = \widetilde{K}P^{-1} \tag{3.11}$$

For the rotary inverted pendulum;

The controllability matrix;

$$M = 1 \times 10^5 \begin{bmatrix} 0 & 0.0003 & -0.0052 & 0.1086 \\ 0 & 0.0004 & -0.0063 & 0.1479 \\ 0.0003 & -0.0052 & 0.1086 & -2.2336 \\ 0.0004 & -0.0063 & 0.1479 & -3.0087 \end{bmatrix} \tag{3.12}$$

The rank of M is 4. In other words, the system is completely controllable. Hence, all poles of the system can be replaced to any desired locations by state feedback.

In the default Quanser setup, the gearbox efficiency and motor efficiency are chosen as 1 when the system's equations are found. However, in this thesis these values are selected from SRV02 manual and these values are shown in Table 2.2.

For the both cases (ideal case and with actual efficiency), the design specifications are chosen same with setup values. According to the setup workbook, [9]

Specification 1: Damping ratio should be 0.7. $(\zeta = 0.7)$

Specification 2: Natural frequency should be 4 rad/s. $(w_n = 4\ rad/s)$

Specification 3: Maximum pendulum angle deflection should be $|\alpha| < 15\ deg$.

Specification 4: Maximum control voltage $|V_m| < 10\ V$.

Specification 5: Two desired poles are chosen at -30 and -40.

The other poles (dominant poles) should be satisfying the damping ratio and natural frequency identifications. Hence, dominant poles can define as:

$$p_1 = -\sigma + jw_d \tag{3.13}$$

$$p_2 = -\sigma - jw_d \tag{3.14}$$

Where w_d is the damped natural frequency and it is calculated as

$$w_d = w_n\sqrt{1-\zeta^2} \tag{3.15}$$

and σ is calculated as;

$$\sigma = \zeta w_n \tag{3.16}$$

Using equations 3.15 and 3.16, the desired locations of dominant poles are found as

$$p_{1,2} = -2.80 \mp j2.86 \tag{3.17}$$

The system and input matrices given in (2.66) and (2.67) aren't in controllable canonical form. Hence, these matrices are transformed into controllable canonical form using transformation matrix P.

Using equation (3.7), (3.8) and (3.9), transformation, new system and input matrices are found. These are;

$$P = 10^3 \times \begin{bmatrix} -1.349 & 0.0167 & 0.0298 & 0 \\ 0 & 0 & 0.0352 & 0 \\ 0 & -1.349 & 0.0167 & 0.0298 \\ 0 & 0 & 0 & 0.0352 \end{bmatrix} \tag{3.18}$$

$$\tilde{A} = \begin{bmatrix} 0 & 1 & 0 & 0 \\ 0 & 0 & 1 & 0 \\ 0 & 0 & 0 & 1 \\ 0 & 750.685 & 99.029 & -17.9098 \end{bmatrix} \tag{3.19}$$

$$\tilde{B} = \begin{bmatrix} 0 \\ 0 \\ 0 \\ 1 \end{bmatrix} \tag{3.20}$$

After the transformation, using the new state space matrices the desired gain matrix is found as

$$\tilde{K} = 10^4 [1.920 \quad 0.8591 \quad 0.1707 \quad 0.0058] \tag{3.21}$$

Using equation (3.11) the original system's gain is found

$$K = [-14.224 \quad 63.587 \quad -6.5397 \quad 7.1702] \tag{3.22}$$

3.2. Routh Hurwitz stability criterion

Routh Hurwitz stability criterion represents the stability condition of system with respect to the characteristic equation of the system. The coefficients of the characteristic equation composed of the Routh Hurwitz table's elements.

If the characteristic equation of the system is defined as

$$D(s) = a_n s^n + a_{n-1} s^{n-1} + \cdots\cdots + a_1 s + a_0 = 0 \tag{3.23}$$

The stability table is:

s^n	a_n	a_{n-2}	a_{n-4}
s^{n-1}	a_{n-1}	a_{n-3}	a_{n-5}
s^{n-2}	b_{n-1}	b_{n-3}	b_{n-5}
s^{n-3}	c_{n-1}	c_{n-3}	n_{n-5}
$\vdots$	$\vdots$	$\vdots$	$\vdots$
s^0	h_{n-1}		

Figure 3.2: *The sample Routh Hurwitz table*

For the first two rows are created from characteristic equation and the other coefficients of rows (in Figure 3.3) are found such as

$$b_{n-1} = \frac{a_{n-1}a_{n-2} - a_n a_{n-3}}{a_{n-1}} = \frac{-1}{a_{n-1}}\begin{vmatrix} a_n & a_{n-2} \\ a_{n-1} & a_{n-3} \end{vmatrix},$$

$$b_{n-3} = -\frac{1}{a_{n-1}}\begin{vmatrix} a_n & a_{n-4} \\ a_{n-1} & a_{n-5} \end{vmatrix},$$

$$c_{n-1} = \frac{-1}{b_{n-1}}\begin{vmatrix} a_{n-1} & a_{n-3} \\ b_{n-1} & b_{n-3} \end{vmatrix},$$

Figure 3.3: *Calculation of the table elements*

According to this theory, for stability, the necessary condition defines as all coefficients must be nonzero and sufficient condition is that coefficients of the characteristic equation should have positive signs. In addition, according to the Routh Hurwitz table, number of unstable poles are found without solving characteristic equation. For stability, the first column of this table should be positive. If there is any sign change in the first column, the number of sign changes will give the number of the instable poles of the system.

In order to determine the stability condition in the genetic algorithm, the gain values of proportional controller are checked by Routh Hurwitz stability criteria. And in the first column of the table should not be sign change.

The characteristic equation of the system is determined as

$$\begin{aligned} D(s) = s^4 &+ s^3(29.8002K_3 + 35.2259K_4 + 17.9098) \\ &+ s^2(29.8002K_1 + 35.2259K_2 + 16.6688K_3 - 6.2510 \times 10^{-14}K_4 \\ &- 99.0298) \\ &+ s(16.6688K_1 - 6.2510 \times 10^{-14}K_2 - 1349.9K_3 - 750.6851) \\ &- 1349.9K_1 \end{aligned} \tag{3.24}$$

The values of first column of Routh Hurwitz table;

$$R_1 = 29.8002K_3 + 35.2259K_4 + 17.9098 \tag{3.25}$$

$$\begin{aligned} R_2 = \big[&(6.25 \times 10^{-14}K_2) - (16.6688K_1) + (1.3499 \times 10^{3}K_3) \\ &+ \big((29.8002K_3) + (35.2259K_4) + 17.9098\big) \\ &\times \big((29.8002K_1) + (35.2259K_2) + (16.6688K_3) - (6.25 \times 10^{-14}K_4) \\ &- 99.0298\big) + 750.6851\big] \\ &\div [29.8002K_3 + 35.2259K_4 + 17.9098] \end{aligned} \tag{3.26}$$

$$\begin{aligned} R_3 = \big[\ &-(\,6.25 \times 10^{-14}K_2) + (16.6688K_1) - (1.3499 \times 10^{3}K_3) \\ &+ (296838677059371K_1\big((29.8002K_3) + (35.2259K_4) \\ &+ (320.7592)\big] \\ &\div \Big[\Big(219902325552 \times (\,6.25 \times 10^{-14}K_2) \\ &- (16.6688K_1)(1.3499 \times 10^{3}K_3) \\ &+ \big((29.8002K_3) + (35.2259K_4) + 17.9098\big) \times (29.8002K_1) \\ &+ (35.2259K_2) + (16.6688K_3) - (6.25 \times 10^{-14}K_4) - (99.0298) \\ &+ (750.685)\Big) - 7.5069 \times 10^{5}\Big] \end{aligned} \tag{3.27}$$

$$R_4 = -1.3499 \times 10^{3}K_1 \tag{3.28}$$

3.3. Genetic Algorithms

Genetic Algorithm is one of the popular meta-heuristic search method that is generally applied to optimization problems of different types design controllers' method. This method is inspired by Darwin's theorem of natural selection. The search starts by composing a population of random potential solutions that are called as chromosomes. The relative success of each chromosome in the population to solve the given optimization problem is called as the fitness of the chromosome. If the fitness value for a chromosome is relatively high that means chromosome is well equipped to solve the optimization problem. After evaluation of the fitness values of each chromosome in the population, a selection procedure is carried out to determine the chromosomes that will contribute to the construction of the new population through genetic operations that are called as crossover, mutation and reproduction. The selection operation is generally based a criterion depending on the fitness of the chromosomes that gives more chance for the chromosomes having relatively higher fitness values. However, sometimes the selection operation can also happen to choose random chromosomes as well. If the selection procedure is carried out wisely, generally the average fitness value of the next population will be greater than the previous one. Besides the best chromosome in the population will probably have the highest fitness value of each chromosome created until that point. This process is carried out for several generations and it is terminated when assumed that the best chromosome is somehow achieved. In this process, three genetic operations and how these three genetic operations are carried out are significant for genetic algorithm. These are selection, mutation and crossover. These genetic operations are milestone to guarantee that the search continuous properly and in general better chromosomes are obtained and selected in new generations.

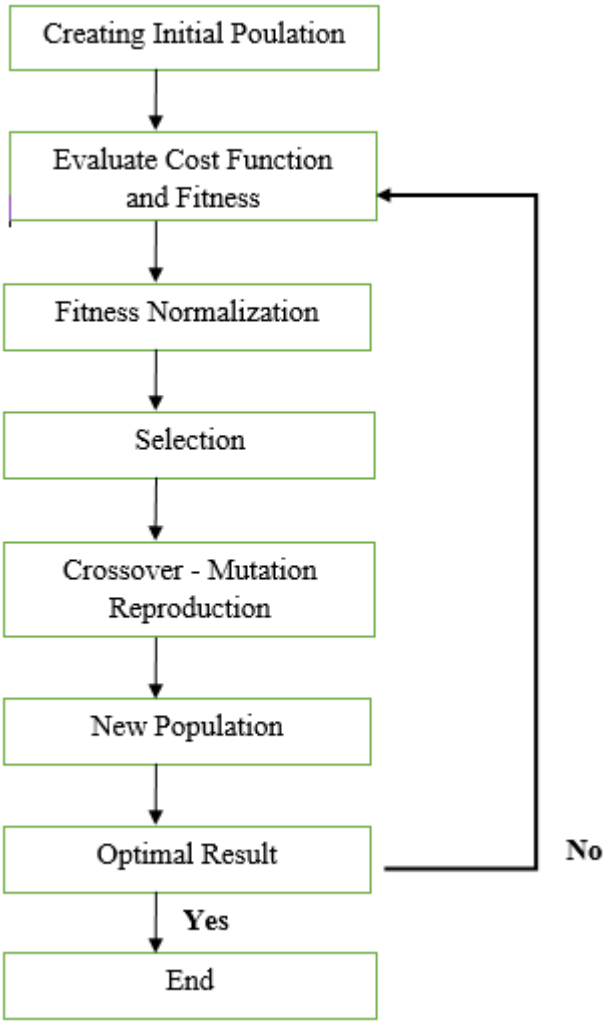

Figure 3.4: *The flow chart of genetic algorithms*

3.3.1 Creating the initial population

Population defines as a subset of solutions in the present generation. Also, it is made up of a group of chromosomes. In order to start the genetic algorithms, initial population is generated randomly for attempted solutions. In this thesis, gain values of controllers are determined as individuals or chromosomes.

A chromosome for the considered optimization problem is a vector with four different state feedback gain values hence it can be formulated as

$$Ch = [K_1 \quad K_2 \quad K_3 \quad K_4] \tag{3.29}$$

Here K_1, K_2, K_3 and K_4 are the genes of chromosome. The definition for K_1, K_2, K_3 and K_4 are given in the beginning of Chapter 3.

Each gene in the chromosomes of the initial population are selected randomly in the range between -100 and 100 with one exception: As we check the R_4 of the Routh Hurwitz array, it seems that in order to have a positive R_4 that is required to have stable closed loop poles as the result of state feedback K_1 value should be negative. Hence the gene K_1 for each chromosome is selected from a range of values between 0 and -100. This process narrows the search space and it will make improve the computation time of the genetic algorithm search.

3.3.2 Cost functions and fitness

In order to measure the competitiveness and achievement of any chromosome to solve the optimization problem a suitable non-negative cost function should be constructed. The cost function penalties the undesired outcomes a chromosome possesses. If more than one condition should be checked during optimization, the cost function should include more than one criterion. For this reason, seven different criteria (conditions) are determined to contribute to the cost function and hence a multi criteria optimization procedure is carried out.

The first four conditions are related with Routh- Hurwitz array. The first column of the Routh Hurwitz array (for the problem it corresponds to 1, R_1, R_2, R_3 and R_4) should all have the same sign (they should all be positive) to guarantee that all the poles of the system after state feedback are replaced in the left open half plane making the system theoretically stable.

Hence R_1, R_2, R_3 and R_4 can be converted into inequalities in the cost function to support stability as:

If $R_1 > 0$ $cost_1 = 0.001 \times |R_1|$ else $cost_1 = 0$ (3.30)

If $R_2 > 0$ $cost_2 = 0.001 \times |R_2|$ else $cost_2 = 0$ (3.31)

If $R_3 > 0$ $cost_3 = 0.001 \times |R_3|$ else $cost_3 = 0$ (3.32)

If $R_4 > 0$ $cost_4 = 0.001 \times |R_4|$ else $cost_4 = 0$ (3.33)

The procedure to determine $cost_1$ to $cost_4$ punishes a potential solution (chromosome) which replaces one or any of the poles to the right half plane, hence makes the system unstable. In other words, if the values of the first column of Routh table are not greater than zero, the chromosome is punished. These four cost functions are necessary to show that the system is stable however they are not sufficient to exactly show the locations of the closed loop poles. Routh Hurwitz only give information of the closed loop system implicitly.

The fifth condition examines the location of the closed loop eigenvalues of the system explicitly and it also checks the relative locations of the eigenvalues based on some relative stability criterion. For these two sub conditions two different cost contributions are measured based on either the chromosome is stable or not.

Sub condition 1: If all the eigenvalues are replaced to the open left half plane, the cost function checks their relative positions of eigenvalues with respect to imaginary axis. If a pole is close to the imaginary axis, it has relatively a higher contribution to the cost function and if a pole is far away from the imaginary axis its contribution to the cost is limited.

When the real parts of all eigenvalues are negative, the condition will be

$$cost_{51} = 0.25 \times \sum_{i=1}^{4} \frac{1}{|real(p_{i)}| + 1} \quad (3.34)$$

Where the real parts of where p_i is the i^{th} eigenvalue of the chromosome. When the real part of at least one eigenvalue is greater than or equal to zero, the condition will be

$$cost_{51} = 0.25 \times \sum_{i=1}^{n} \left| real(p_i) \right| + n \tag{3.35}$$

Where n is the number of eigenvalues that are in the right half plane, p_i is the value of the i^{th} eigenvalue in the right half plane.

Sub condition 2: $Cost_{51}$ in its current shape only considers the position of the poles with respect to imaginary axis, however if a stable eigenvalue is very close to the imaginary, in practical applications it has potential to make the system unstable. For this reason, to guarantee that all the stable eigenvalues are relatively away from the imaginary axis a new cost contribution is also added as an extra term. For this reason, the eigenvalues which are between the imaginary axis and s=-2 line in s-plane are further punished. Hence for a chromosome which has stable eigenvalues

$$cost_{52} = 0.25 \times \sum_{i=1}^{k} real(m_i) + k \times 0.5 \tag{3.36}$$

Where k is the number of eigenvalues which reside between the imaginary axis and s=-2 line of s-plane and m_i is the value of the corresponding eigenvalue.

The term $cost_{52}$ evaluated for a stable chromosome should also be calculated for an unstable chromosome to balance the effect of punishment. The maximum value of $cost_{52}$ for a stable chromosome can be equal to 2 hence a punishment cost of two units is also added to $cost_5$ for unstable chromosomes using

$$cost_{52} = 2 \tag{3.37}$$

Finally, $cost_5$ is calculated for some of the applications only accounting $cost_{51}$ hence for these applications:

$$cost_5 = cost_{51} \tag{3.38}$$

For the remaining applications the relative stability sub condition is also considered hence for these remaining applications $cost_5$ is calculated using,

$$cost_5 = cost_{52} \tag{3.39}$$

The sixth condition is linked with total values of gains of restriction. Absolute values of gains should be equal or less than some total values. These total values selected as 30,60,90 and 120. If the summation of gain values is greater than total value, the condition is defined as

$$|K_1| + |K_2| + |K_3| + |K_4| \geq total\ value$$

$$cost_6 = cost_6 + 0.01 \times (|K_1| + |K_2| + |K_3| + |K_4|) - total\ value \tag{3.40}$$

The last condition is correlated with absolute values of real and imaginary parts of eigenvalues. If a stable poles has some imaginary parts, the imaginary part/absolute (real part) ratio should be smaller than a threshold value in order to minimize the effect of undamped oscillations. If the absolute value of real parts is four times less than absolute value of imaginary part, the condition will be,

$$cost_7 = cost_7 + 0.01 \times (4 \times |(imaginary\ part)| - |(real\ part)|) \tag{3.41}$$

The total cost function is defined for different four cases. For all case, the first four conditions are common. In case one, dominant poles and ratio of imaginary part /real part conditions are neglected. Then the cost function defined as for case one,

$$total\ cost = cost_{1-4} + cost_{51} + cost_6 \tag{3.42}$$

In case two, only dominant pole condition does not be included and the cost function defined as;

$$total\ cost = cost_{1-4} + cost_{51} + cost_6 + cost_7 \tag{3.43}$$

For the last two cases, case one and case two are examined again with the dominant pole case condition.

$$total\ cost = cost_{1-4} + cost_{51} + cost_{52} + cost_6 \tag{3.44}$$

$$total\ cost = cost_{1-4} + cost_{51} + cost_{52} + cost_6 + cost_7 \quad (3.45)$$

The fitness function is depicted as a function which the algorithm tries to optimize. It is an essential part in genetic algorithms because the fitness function tests the candidate solutions and measures each candidate solutions' ability to solve the optimization problem.

Fitness can be defined in many ways. However, for the sake of simplicity in the simulations for all cases it is defined as

$$fitness = \frac{1}{total\ cost} \quad (3.46)$$

3.3.3 Fitness normalization

Fitness normalization is necessary in order to define the relative fitness values of each individual (chromosome) with respect to each other. For that reason, the fitness values of each individual is recalculated by dividing the fitness values by the summation of fitness values of each individual in the generation. Therefore, after this normalization process, the summation of all fitness values becomes 1.

3.3.4 Selection

Selection is the mechanism to choose chromosomes for genetic operators with generally based on the fitness function. In this thesis, the most common selection approach, Roulette Wheel, is used. According to this approach, population is located on the roulette wheel based on their normalized fitness values. The portion of each section is correlated with the normalized fitness value of the corresponding chromosome. In other words, the fittest individuals have large portions and the weakest individuals have smallest portions in the roulette wheel.

Therefore, the individual with the largest portion in the roulette wheel has the highest probability to be selected for the genetic operations and the individuals ordered after the fittest individual have slightly less probability to be selected for the genetic operations with the least fit individual having the worst selection chance for the genetic operations.

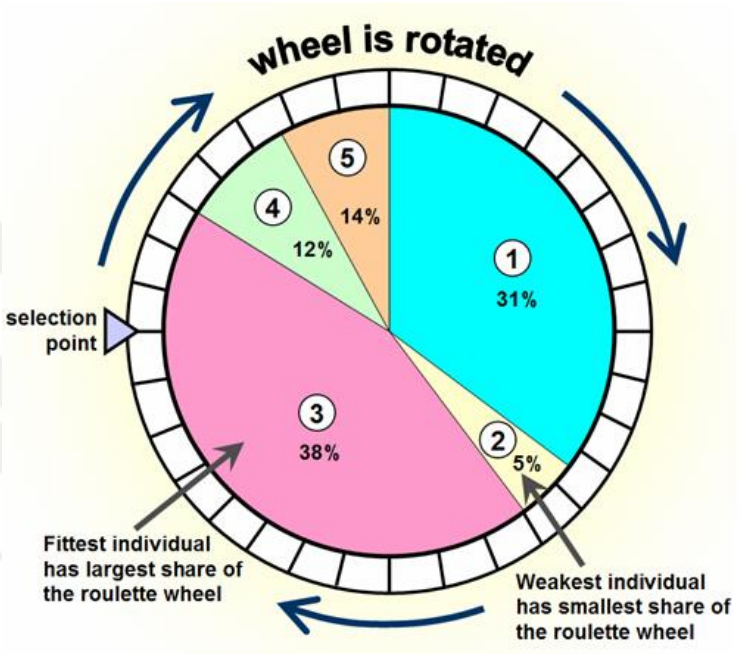

Figure 3.5: *The roulette wheel approach*

[13]

3.3.5 Crossover and mutation reproduction

Crossover is similar to biological crossover procedure. Hence, the crossover in genetic algorithm is defined as a method of recombination and knowledge transfer between two selected adult chromosomes to yield two new offspring (chromosomes generated for next generation). Generally, crossover can be handled by different methods: either some genes of the adult chromosome are exchanged or some genes of the adult chromosomes generated by linear interpolation. In genetic algorithms, mutation is defined as a random deformation in a single chromosome (a simple or multiple gene modification), of with a certain probability.

In this thesis, the adult chromosomes for crossover operation are determined with mixed selection procedures. The first half of chromosomes are chosen with respect to their fitness values using roulette wheel selection.

The other half of the chromosomes are selected as a mixture of random selection and roulette wheel selection where the abundance of the chromosomes in this half are chosen by roulette wheel selection and only 5 of the chromosomes are selected randomly.

Mutation and reproduction procedures are applied randomly however in reproduction the elitism method is also applied (the fittest chromosome of the current generation is directly inserted into next generation)

3.4 Genetic Algorithm's parameter

In all the simulations the genetic algorithm search parameters are presented in Table 3.1 for genetic algorithms.

Table 3.1: *Genetic Algorithm's parameters*

Population Size=200	Number of Chromosome =400
Number of Variables (Genes)=4	Ratio of Crossover=0.9
Number of Generation=500	Ratio of Reproduction=0.06
Ratio of Mutation=0.04	

CHAPTER 4

SIMULATION AND EXPERIMENTAL RESULTS

In this chapter, genetic algorithm optimization results for different simulation are tabulated. The optimization results give the gain values and corresponding eigenvalues as the result of state feedback control. Then in real time applications, these gain values are used in hold mode of the rotary inverted pendulum and the performance of corresponding real time applications are compared with the default state feedback computation. In real time application some of the gain values obtained as the result of optimization process are not able to keep the pendulum in hold mode. However, some of the gain values managed to keep the pendulum at upright position. For the gain values where the real time application becomes successful corresponding arm angle (θ), pendulum angle (α) and applied voltage waveforms are drawn. The main mechanism that makes some of the real time application successful and some unsuccessful seems to be the total absolute gain values in the optimization simulations. When total absolute gain value is limited to 30 (means extra penalty is given to the chromosomes that passes this limit value), for all four cases given by the cost equations 3.42, 3.43, 3.44, 3.45, the pendulum is not able to pass from swing up mode to hold mode successfully. What is observed is the pendulum makes a full cyclic turn, tries to get into hold on mode once again by speeding up and generally hits the corner of the set up and restarts swing up mode of operation. When the total absolute gain value is limited to 60, only one case is unsuccessful (given by the cost equation 3.44). When the total absolute gain value is limited to 90, the pendulum is successful only one case (given by cost equation 3.45). And finally when the total absolute gain value is 120, two cases are successful (given by cost 3.43 and 3.45)

After this step, the most successful genetic algorithm and default setup results are once again tested for reference signal tracking due to different type of reference changes in arm

angle in steady state conditions and application of disturbance that increases the arm's mass.

4.1. Experimental results

4.1.1 Default result

Gain values are defined in setup manual as a

$$K = [-5.2612 \;\; 28.1568 \;\; 2.7576 \;\; 3.2190]$$

These gain values are obtained when the motor efficiencies are taken as 1 and these gain values are assumed to replace the eigenvalues of the system to locations -30, -40 and 2.80±j2.86. When these gain values are used in state feedback in hold mode of operation in real time application, the corresponding arm angle, pendulum angle and applied voltage plots are obtained in Figure 4.1, 4.2 and 4.3 respectively.

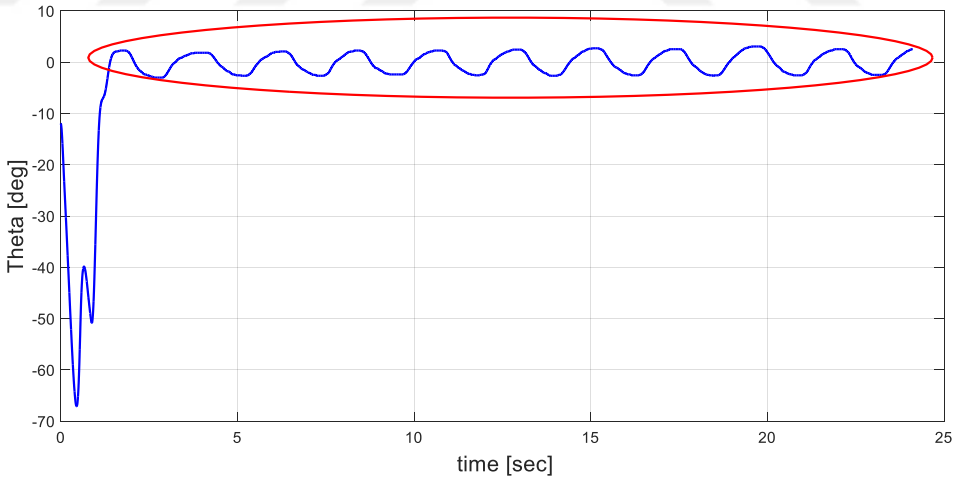

***Figure 4.1**:The arm angle of setup*

To observe the oscillation, Figure 4.1 is zoomed out and this area shows in Figure 4.1.1

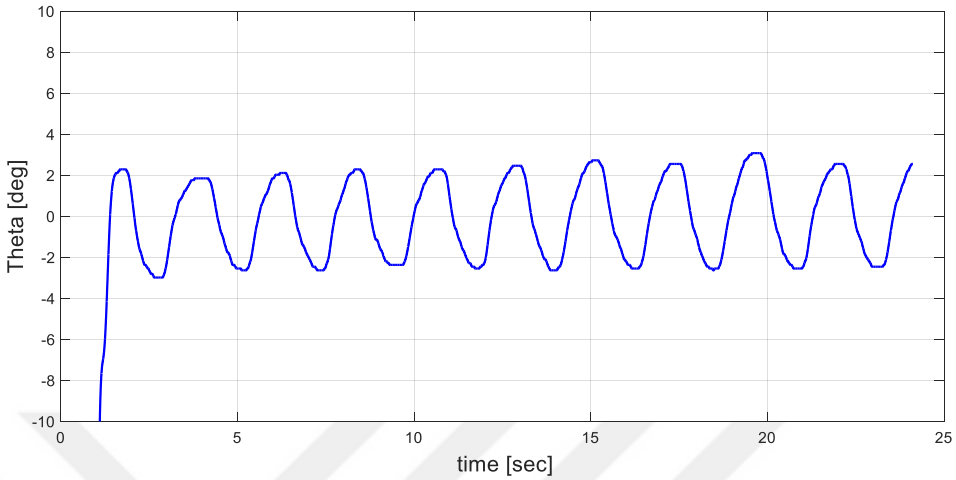

Figure 4.1.1: *The oscillation in the pendulum angle*

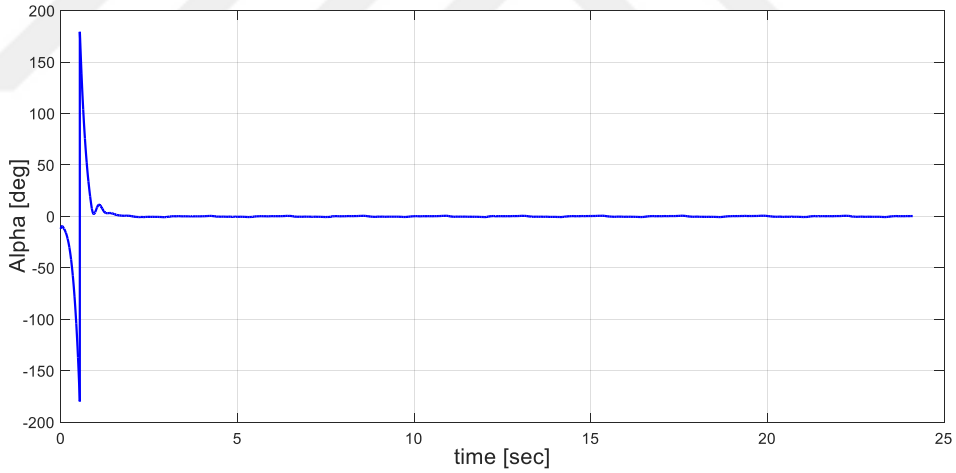

Figure 4.2: *The pendulum angle of setup*

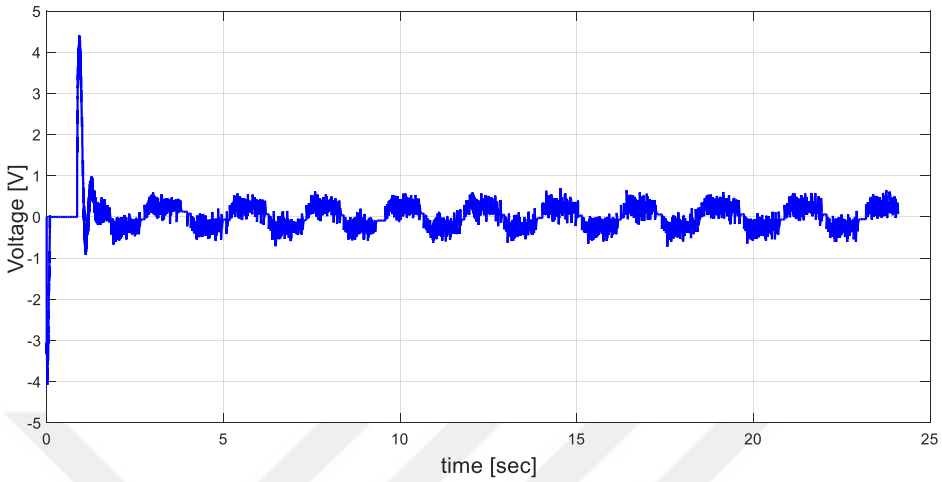

Figure 4.3: *The voltage of setup*

All the plots are drawn only after the pendulum controller enters to hold mode of operation for the first time. As seen from Figure 4.2, the pendulum first enters the hold mode of operation but it cannot stabilize in hold mode at first step and then it returns back to swing up mode and makes a cyclic turn of 360 degrees (the switch between 0 to -180 degree, the jump from -180 degree to 180 degrees and the drop from 180 degrees to nearly 0 degree in the first 2-3 seconds of the figure) and then finally stabilizes at the second step. The pendulum stabilizes at the unstable equilibrium point.

However, in Figure 4.1 and Figure 4.1.1 some oscillations are observed around the reference set point ($\theta = 0$ degrees). These oscillations are not at desired levels however they keep the pendulum at upright position. (Oscillation degree is ± 2 degree) In Figure 4.3, except for the transient situations where the system turns from swing up mode to hold mode, it seems the applied voltage levels are staying in desirable ranges (in the figure only the voltage levels at hold mode of operation are shown).

4.1.2 State feedback result

When the efficiencies of the motor are taken from Table 2.2, the gain values that should be applied at state feedback control to replaces the eigenvalues of the system to -30, -40, -2.80±j2.86 are calculated as

$$K = [-14.224 \quad 63.587 \quad -6.5397 \quad 7.1702]$$

When these gain values are used in state feedback in hold mode of operation in real time application, the corresponding arm angle, pendulum angle and applied voltage plots are obtained in Figure 4.4, 4.5 and 4.6 respectively.

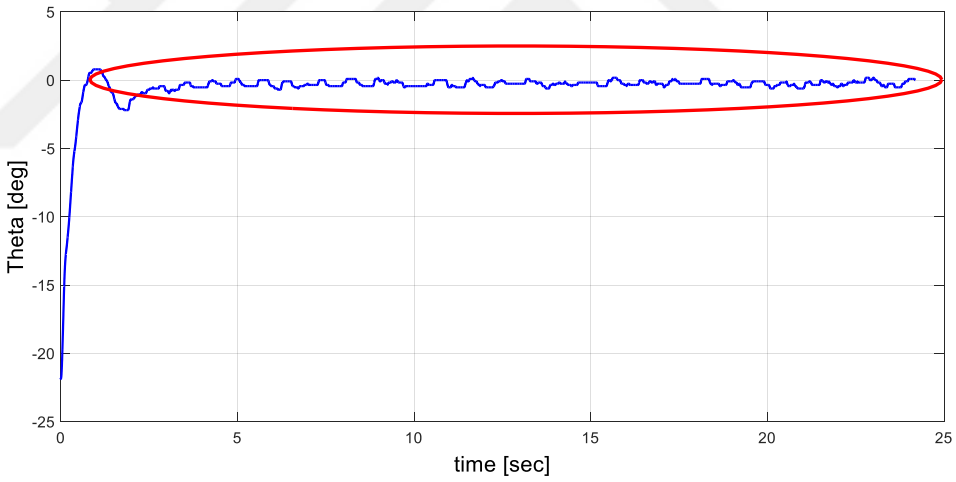

Figure 4.4:*The arm angle for state feedback controller*

To observe the oscillation, Figure 4.4 is zoomed out and this area shows in Figure 4.4.1

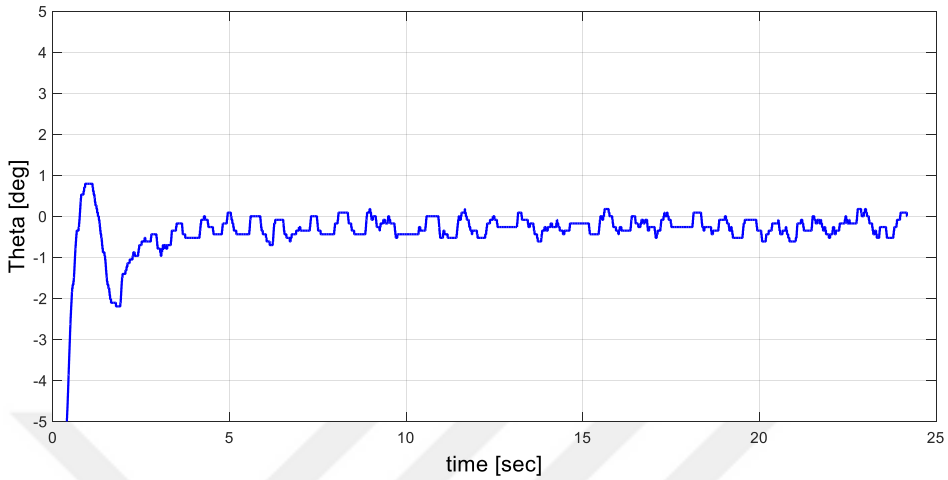

Figure 4.4.1: *The oscillation in the pendulum angle*

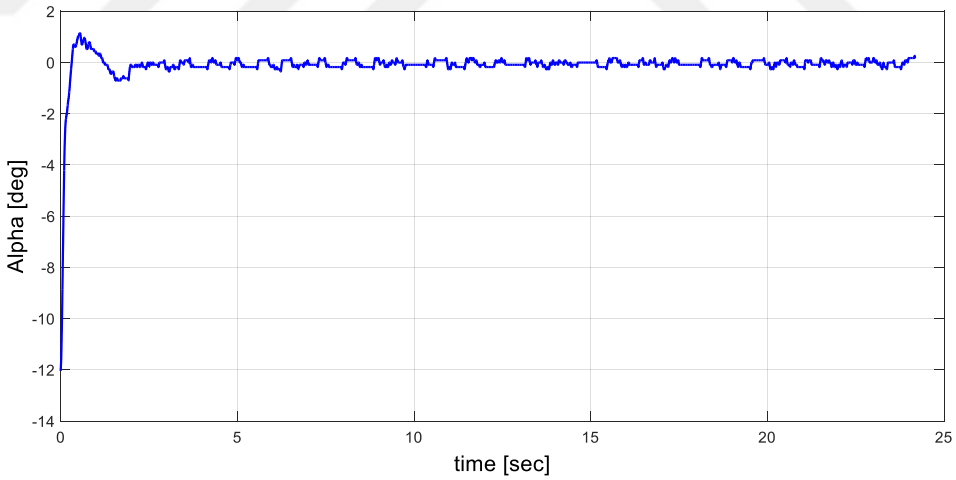

Figure 4.5:*The pendulum angle for state feedback controller*

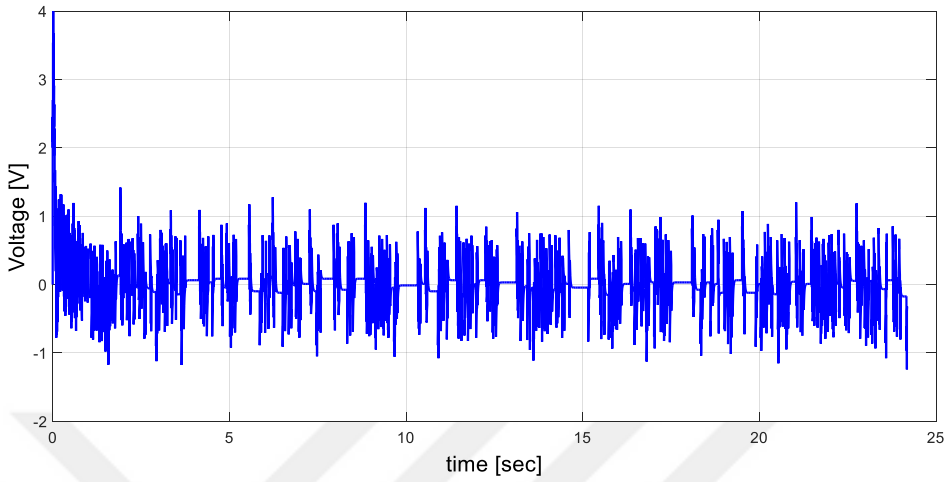

Figure 4.6:*The voltage for state feedback controller*

Accordance with Figure 4.4 and Figure 4.4.1 although the oscillation is observed, its range is smaller than default setup values. (Oscillation range is between 0° and -1°) The second component of the gain value (K_2=63.587) of pendulum angle is almost three times higher than the same gain component of the default set up. Hence, high gain value at this component seems to create the vibration. Besides, for both state feedback configurations eigenvalues satisfy the desired pole locations which are found in Chapter 3.

4.1.3 Genetic Algorithm results

The gain values and eigenvalues are tabulated for each case and they are presented in Table 4.1, Table 4.2, Table 4.3 and Table 4.4, respectively and between Figure 4.7 and Figure 4.24 show three parameters in graphically.

Table 4.1: *Gain values and eigenvalues for case 1*

Total gain limit	K	Eigenvalues
30	[-3.3574 22.2601 -4.7755 4.5875]	-25.8170; -5.2570±13.225i; -0.8667
60*	[-6.9181 45.5623 -4.7962 5.7963]	-60.5832; -12.385; -3.1321±1.6236i
90	[-11.5339 51.0750 -14.1884 13.0375]	-37.0866; -8.1808±19.9495i; -0.9030
120	[-19.8067 69.5498 -15.4636 14.2932]	-32.1925; -1.5146 -13.4375±19.1722i

Associated with Table 4.1, all four conditions have complex eigenvalues. Apart from the result with total gain limit is 60, the imaginary parts of complex eigenvalues have high value. And dominant poles are very close to imaginary axis. Among these result only condition 2 where the absolute gain is limited with 60 is successful. What is observed in condition 2 its dominant pole is more away from the imaginary axis with respect to dominant poles of other conditions.

" * " represents the succesful conditions in each case

Table 4.2: *Gain values and eigenvalues for case 2*

Total gain limit	K	Eigenvalues
30	[-6.7941 52.5941 -8.5575 8.5723]	-25.6137; -19.6845; -18.5846;-0.9788
60*	[-4.2142 41.0792 -4.0519 5.6020]	-80.9256; -6.6712; -4.6205; -2.2805
90	[-12.1542 58.2901 -8.6790 8.7829]	-37.2222; -14.7065±1.216i; -2.0241
120*	[-11.1376 70.4842 -7.6880 9.6869]	-113.8569; -8.0871; -4.2462; -3.8452

According to the Table 4.2 all eigenvalues except the condition where the total absolute gain limit value equals 90 are real and still in this condition the absolute imaginary part to absolute real part ratio is low due to cost function 3.43. Except for the first condition where the gain limit is 30, dominant poles are comparably away from the imaginary axis. Among these results the second and the fourth conditions are successful, the first and the third conditions are unsuccessful.

" * " represents the succesful conditions in each case

Table 4.3: *Gain values and eigenvalues for case 3*

Total gain limit	K	Eigenvalues
30	[-16.3777 43.4141 -9.9133 9.0397]	-27.9306; -2.0194; -5.4865±19.0225i;
60	[-14.4045 52.7235 -20.3744 21.7687]	100×(-1.7273; -0.0075; -0.0205±0.1207i)
90	[-22.3198 50.6343 -13.0103 12.2167]	-50.8915; - 1.9994; -3.8268±16.7765i;
120	[-16.5060 41.7552 -5.7214 5.5727]	-11.0012±8.2449i; -10.8560±0.1871i

Table 4.4: *Gain values and eigenvalues for case 4*

Total gain limit	K	Eigenvalues
30	[-21.0713 86.6592 -14.2016 13.8867]	-47.8376; -2.0007; -17±2.7633i
60*	[-13.9091 77.1822 -10.3866 11.2741]	-82.8702; -2.0; -10.3285±2.5701i;
90*	[-6.4366 61.7867 -5.6803 8.8923]	-150.2543; -4.1609; -3.8503;-3.6094
120 *	[-11.9264 77.7633 -8.6061 10.4792]	-112.3599; -10.7552; -4.5285;-2.9418

" * " represents the succesful conditions in each case

According to the Table 4.3, for condition 1 there is a slightly dominant pole however the complex conjugate poles have slightly high imaginary parts and that makes the system prone to oscillatory behavior. For condition 2, the dominant pole is very close to the imaginary axis. Condition 3 represents similarities with condition 1 and interestingly condition 4 has no dominant poles with one complex conjugate pair eigenvalues having imaginary part values being slightly close to the real part values. None of the corresponding conditions are able to successfully hold the pendulum. None of the conditions in Table 4.3 are able to hold the pendulum successfully. For that reason, real time applications of pendulum angle, arm angle and applied voltage don't be given in this case.

In Table 4.4, all eigenvalues for each condition are at the left side of s= -2. In real time application except for the condition where absolute gain limit is 30, all conditions manage to keep the pendulum in upright position. However, condition will cause of some oscillation in second component of the gain values in each condition appears to be very big. In addition, all dominant poles are close to -2. Hence, the effect of dominant poles is reduced and the pendulum gets into steady state more rapidly. The figures of arm angle pendulum angle and applied voltage for successful real time applications are given starting from Figure 4.7 to Figure 4.24.

For case 1, only total absolute gain value limitation 60 condition is graphed and real time applications are given Figure 4.7 to Figure 4.9

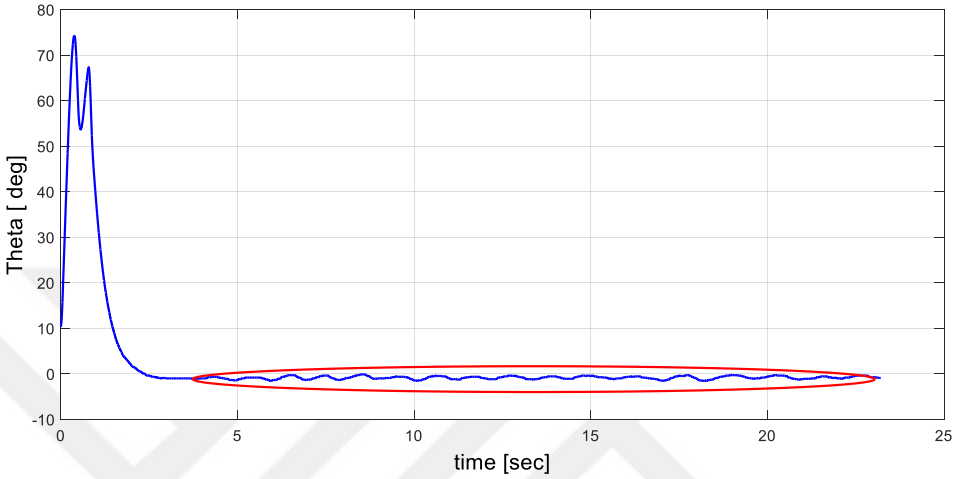

Figure 4.7:*The arm angle when total gain value=60 for case 1*

To observe the oscillation, Figure 4.7 is zoomed out and this area is shown in Figure 4.7.1.

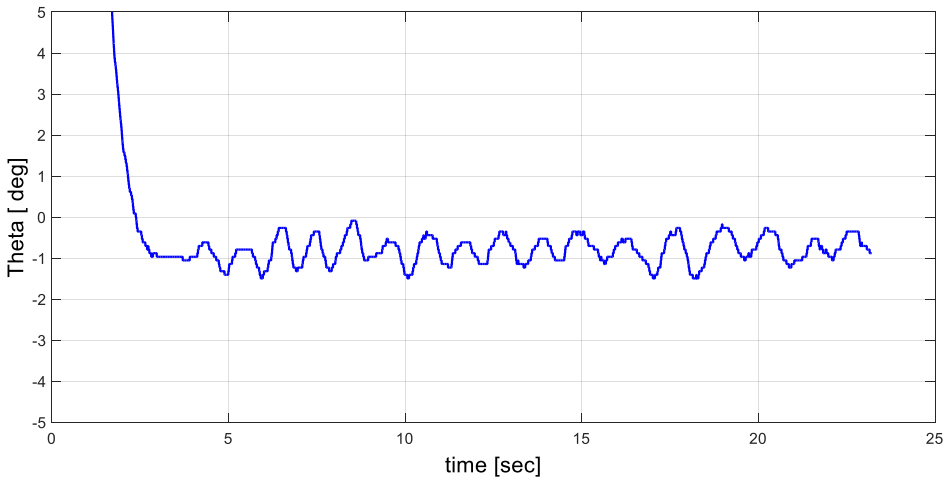

Figure 4.7.1:*The oscillation in the arm angle*

The oscillation range is between 0 and -1 degrees. This range is smaller than default condition.

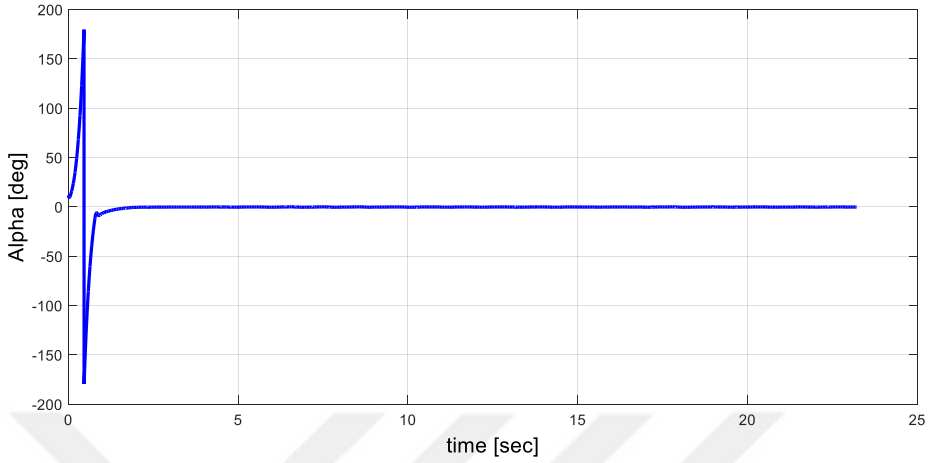

Figure 4.8: *The pendulum angle when total gain value=60 for case 1*

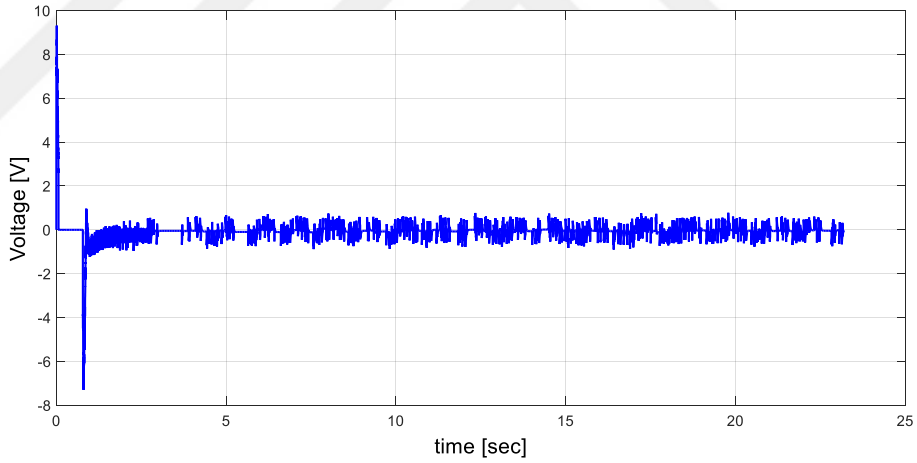

Figure 4.9: *The voltage when total gain value=60 for case 1*

For the case 2, total absolute gain value=60 and total absolute gain value=120 conditions are successful. Therefore, their real time applications are given Figure 4.10 to Figure 4.15

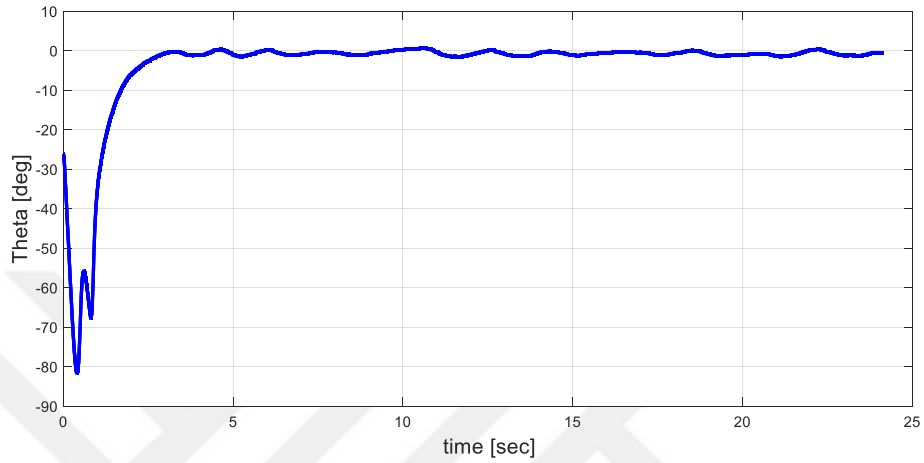

Figure 4.10: *The arm angle when total gain value=60 for case 2*

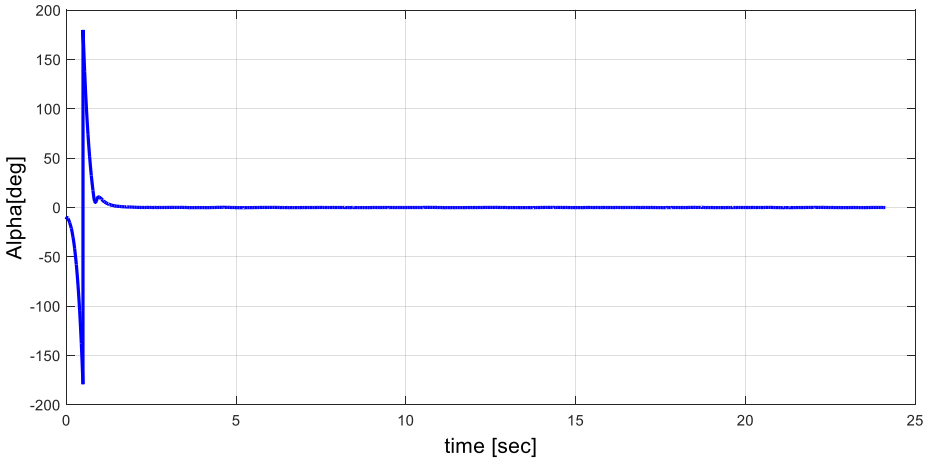

Figure 4.11: *The pendulum angle when total gain value=60 for case 2*

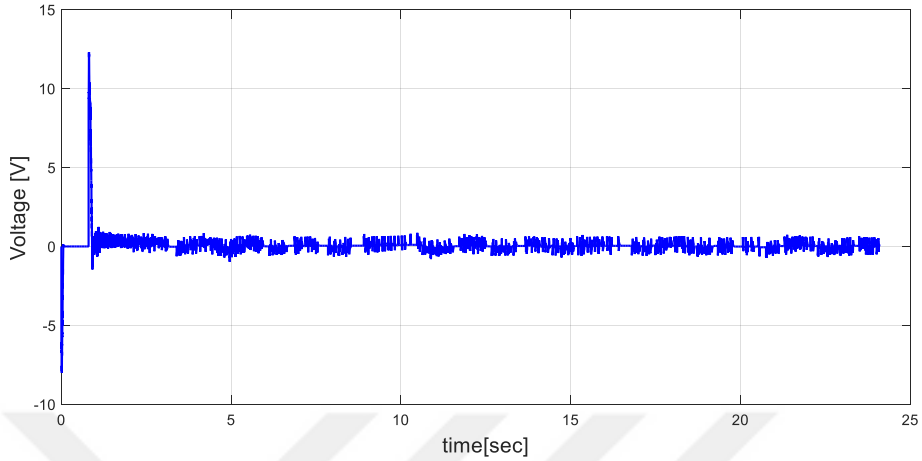

Figure 4.12: *The voltage when total gain value=60 for case 2*

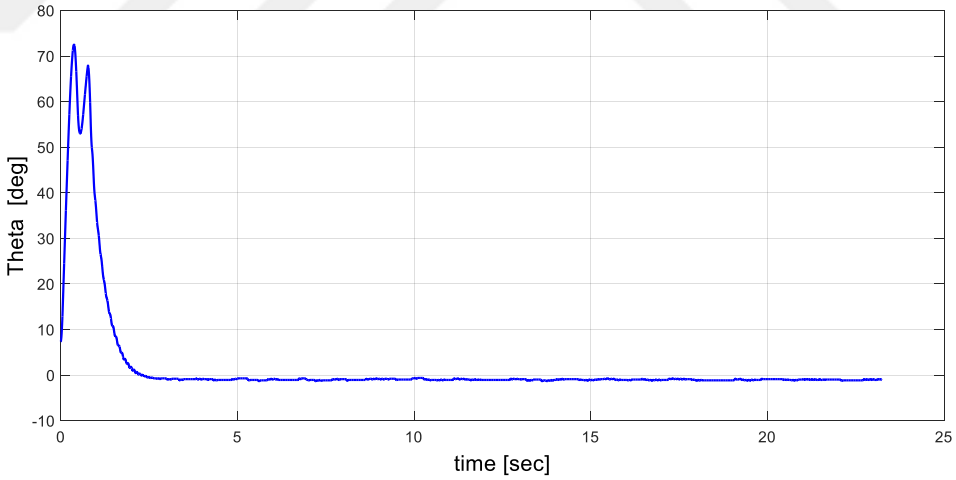

Figure 4.13 *The arm angle when total gain value=120 for case 2*

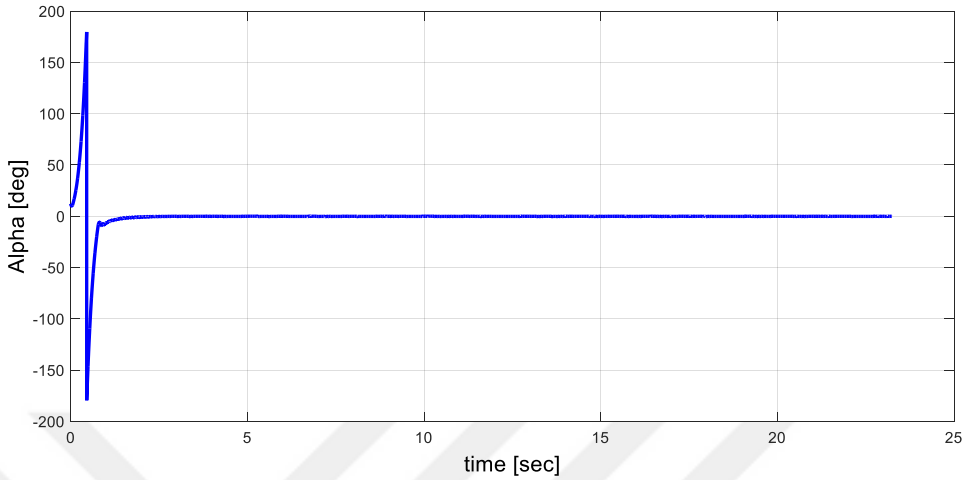

Figure 4.14: *The pendulum angle when total gain value=120 for case 2*

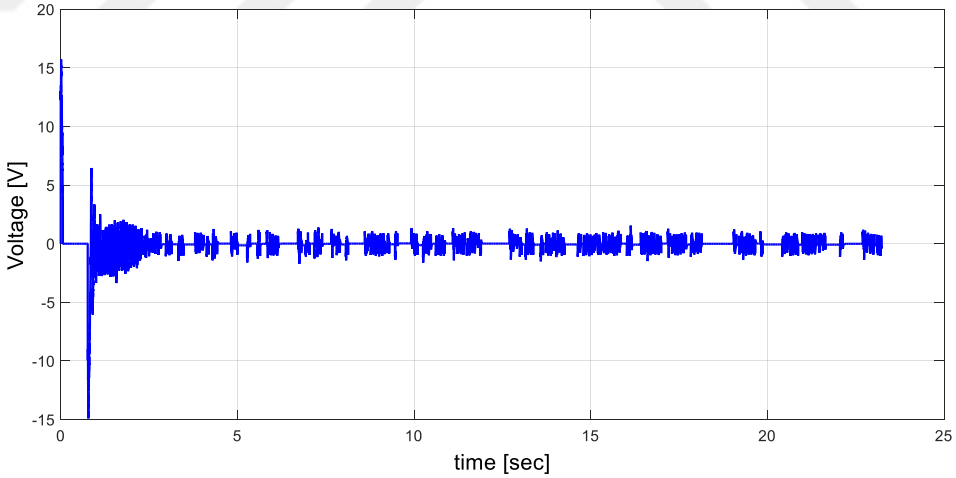

Figure 4.15: *The voltage when total gain value =120 for case 2*

For the case 4, total absolute gain value=60, total absolute gain value=90 and total absolute gain value=120 conditions are successful. Therefore, their real time applications are given Figure 4.16 to Figure 4.24

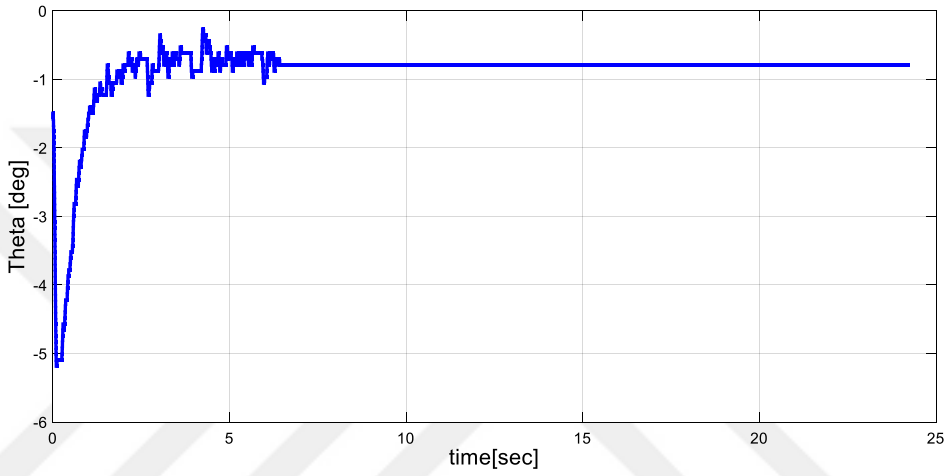

Figure 4.16: *The arm angle when total gain value=60 for case 4*

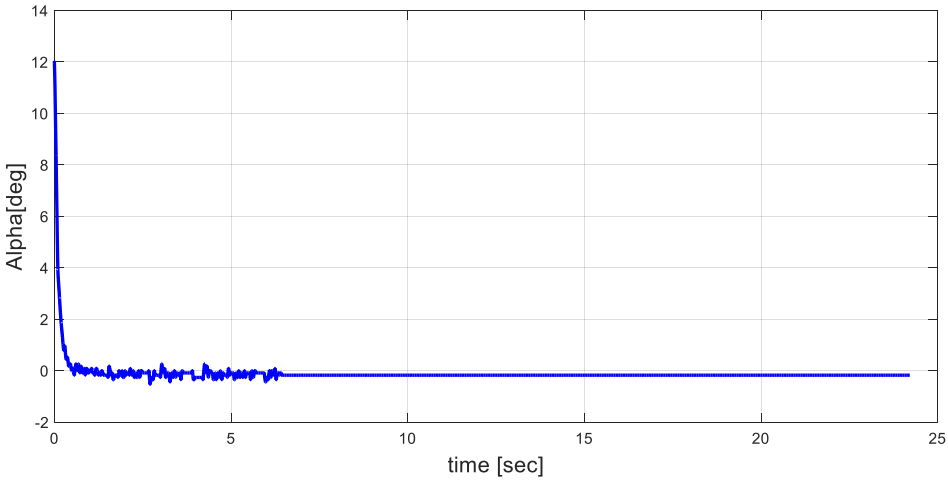

Figure 4.17: *The pendulum angle when total gain value=60 for case 4*

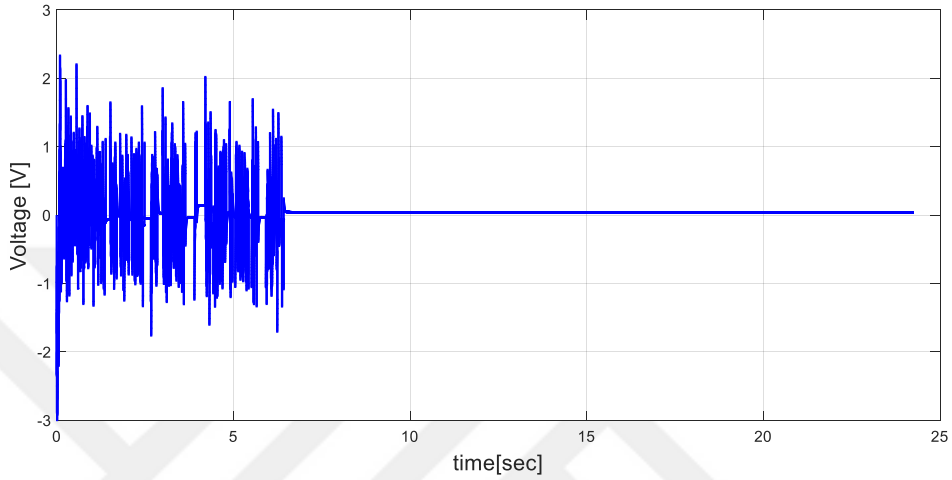

Figure 4.18: *The voltage when total gain value=60 for case 4*

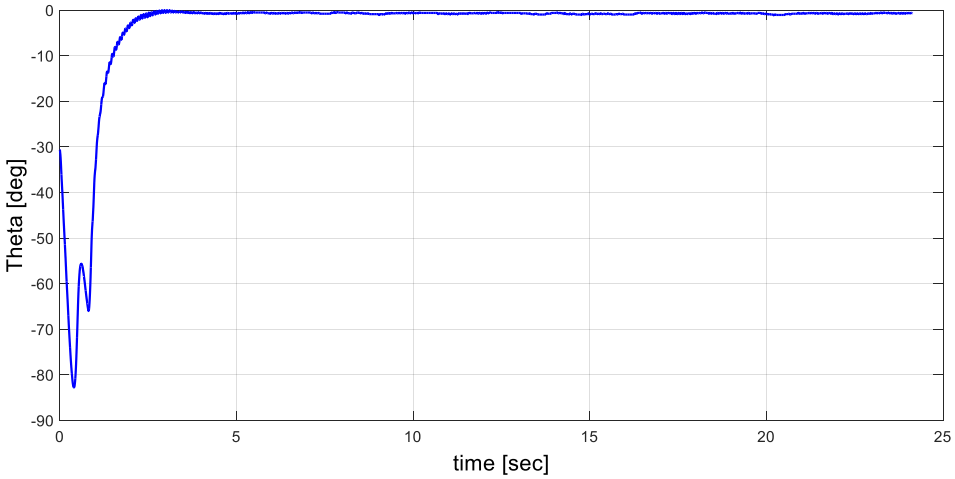

Figure 4.19: *The arm angle when total gain value=90 for case 4*

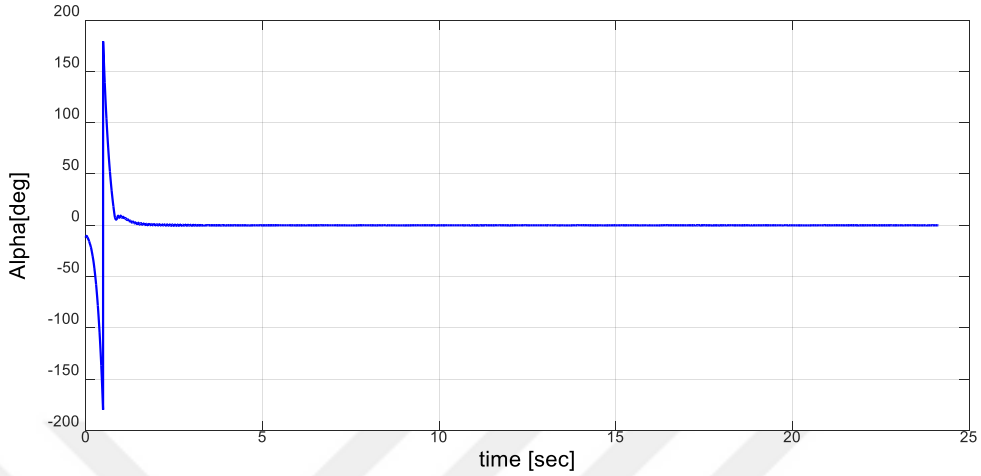

Figure 4.20: *The pendulum angle when total gain value=90 for case 4*

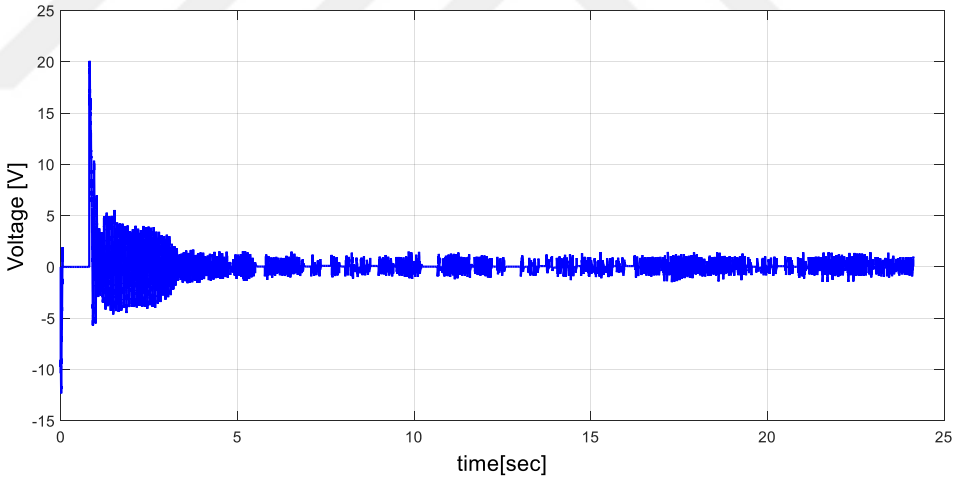

Figure 4.21: *The voltage when total gain value=90 for case 4*

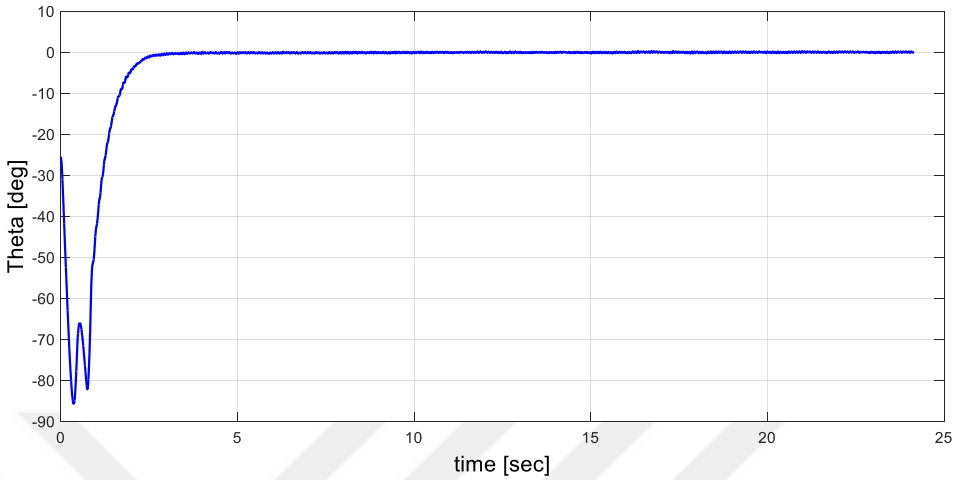

Figure 4.22: *The arm angle when total gain value=120 for case 4*

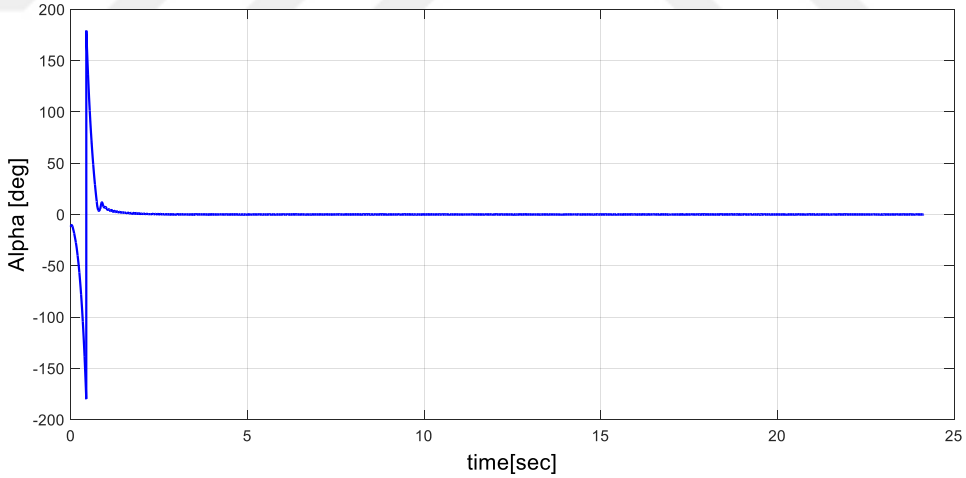

Figure 4.23: *The pendulum angle when total gain value=120 for case 4*

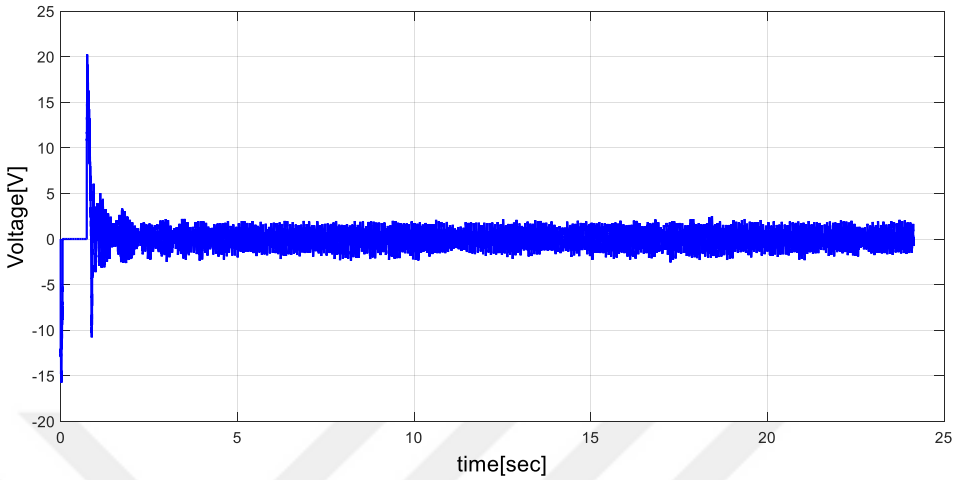

***Figure 4.24**: The voltage when total gain value=120 for case 4*

Compared with the results of 4.1.1 and 4.1.2 the genetic algorithm methods provide better solution even if some oscillation and vibration are also observed in these results. However, in the genetic algorithm results, these side effects are comparably removed at some extent.

K_2 gain value is related with pendulum angle. As K_2 gain value gets higher we generally observe unsuccessful transition from the swing up mode to hold mode of operation that produces unsuccessful hold mode of operation.

This can be due to other parameters of the swing up mode of operation such as the epsilon value which represents the threshold pendulum angle value when the controller passes from swing up mode to hold mode. Epsilon is nearly ± 12 degrees and in the transition from swing up mode to hold mode that K_2 is multiplied with ± 12 degrees in state feedback operation and this occasion probably produces very significant applied voltage component to the system which can make the pendulum move rapidly when it is nearly in upright position.

In real time applications, one interesting thing has happened. That is observed in case 4 when the total absolute gain value is limited to 60. The pendulum stayed in upright position motionless ($\alpha=0°$) after a transient period and after that no oscillations are observed. (in Figure 4.16, Figure 4.17 and Figure 4.18)

4.2 Reference input tracking capability

The reference input tracking capabilities of the controllers is a significant test for concluding whether the controllers are working properly or not. For this reason, some real time reference signal tracking applications are proposed. The system performance is tested in the existence of square and sinusoidal reference signals applied to arm angle (θ) with frequencies of 0.1 and 0.5 Hertz and with an amplitude of 1 (1 degrees). When the frequency is 0.5 Hertz, in of the applications, the amplitude of the reference signal is taken as 2 degrees. For this purpose, default values, the result in state feedback controller and some cases in genetic algorithm is tested. All results are shown in graph and in these graphs, the real time applications present between 10^{th} and 30^{th} seconds. In other words, only hold positions are graphed. In these graphs reference input signal compares to arm angle.

4.2.1 Default results

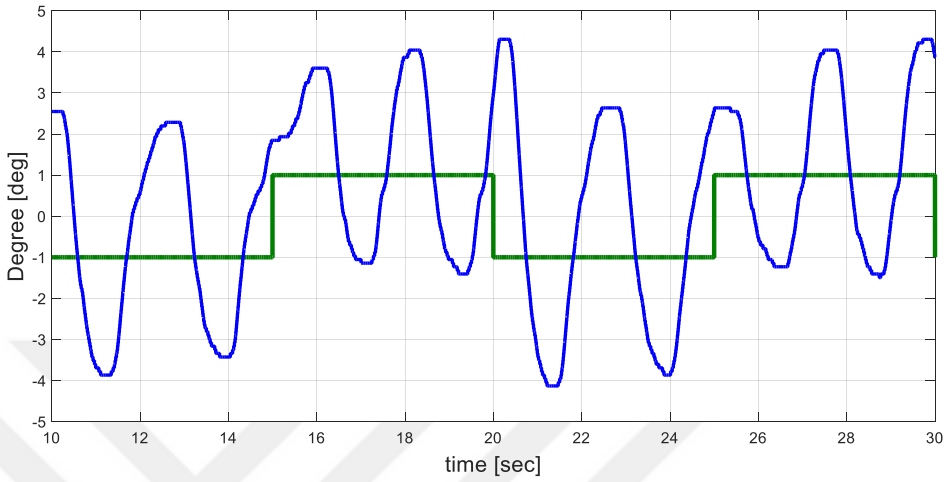

Figure 4.25:*The reference signal in square wave (green) and the arm angle of the system (blue) when f=0.1 Hz*

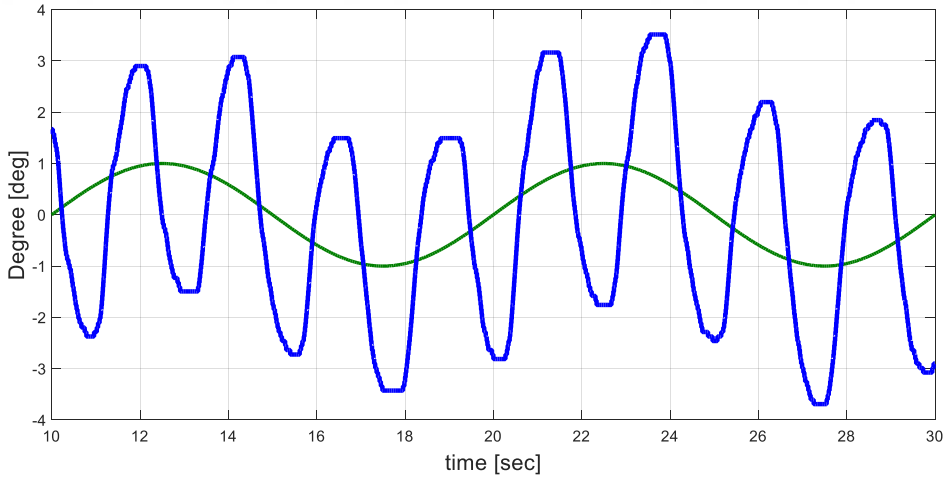

Figure 4. 26: *The reference input(green) in sinusoidal wave, the arm angle of the system (blue) when f=0.1 Hz*

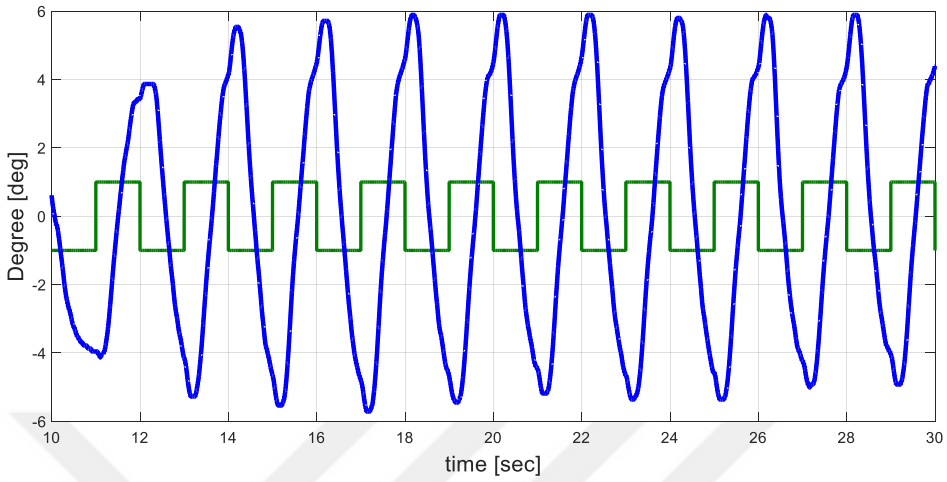

Figure 4.27: *The reference signal in square wave* (green) *and the arm angle of the system* (blue) *when f=0.5 Hz*

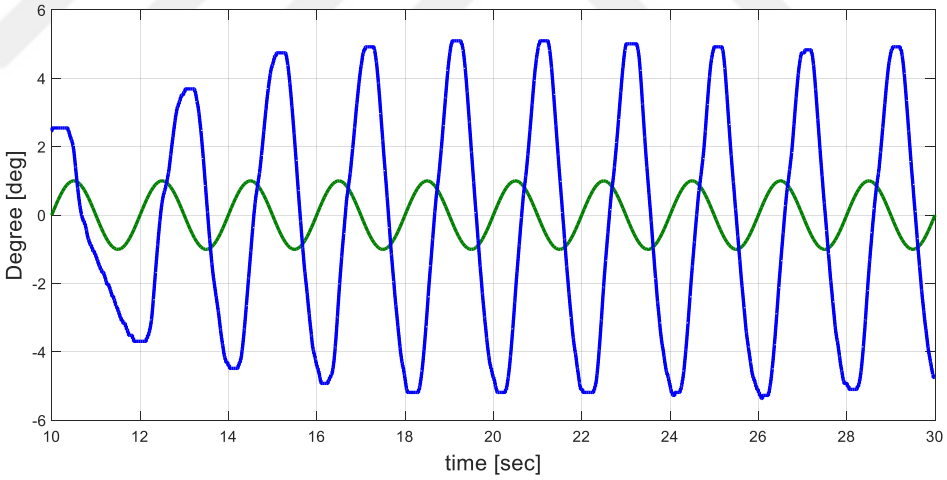

Figure 4.28: *The reference input* (green) *in sinusoidal wave, the arm angle of the system* (blue) *when f=0.5 Hz*

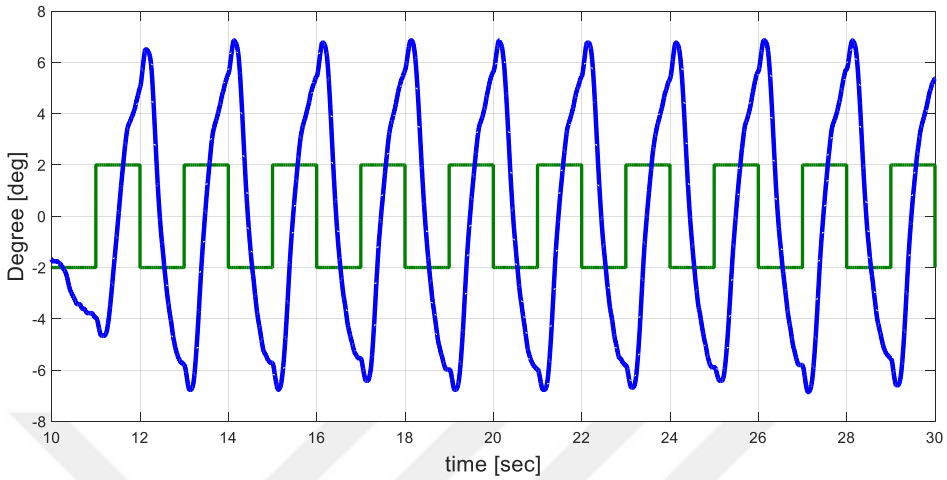

Figure 4.29: *The reference signal in square wave (green) and the arm angle of the system (blue) when f=0.5 Hz with amplitude =2*

As it can see that, from Figures 4.25 to Figure 4.29, the difference between the reference signal and degree of the arm angle is high. Hence, default controller cannot track the reference input signals very well.

4.2.2 State feedback results

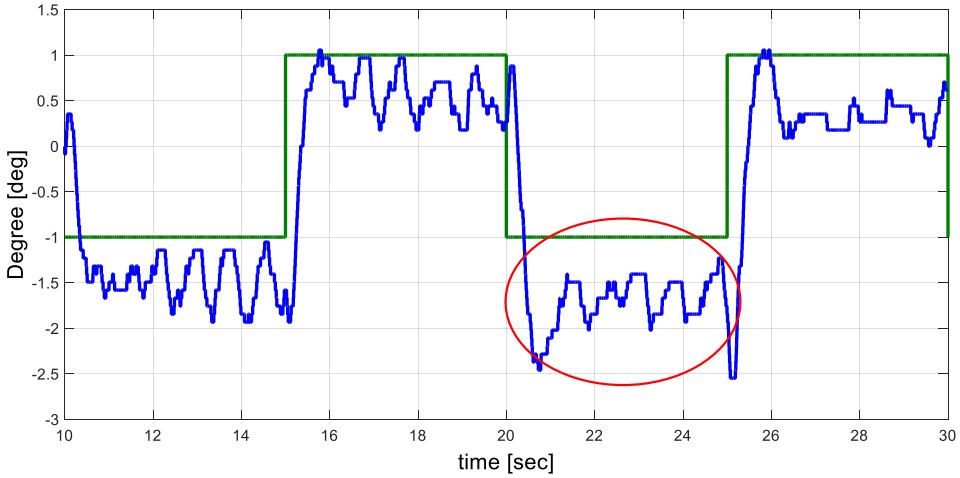

Figure 4.30: *The reference signal in square wave (green) and the arm angle of the system (blue) when f=0.1 Hz*

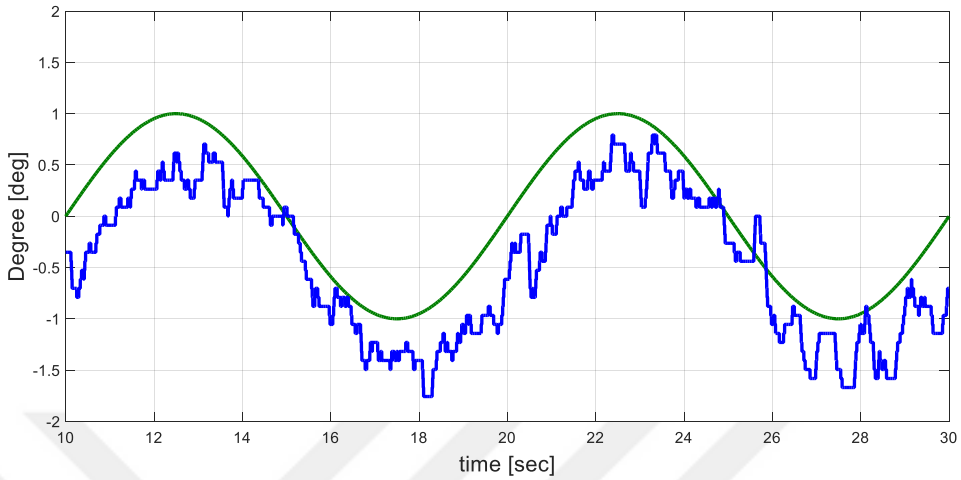

Figure 4.31: *The reference signal in sinusoidal wave (green) and the arm angle of the system (blue) when f=0.1 Hz*

The state feedback is only drawn for reference signals that has 0.1 Hertz frequency and an amplitude of 1 degree as the other reference signal tracking applications terminated unsuccessfully. In 0.1 Hertz, in Figure 4.31 the maximum difference in reference input and arm angle degree is 1.5 degree. This difference is shown in red ellipse. However, in low frequency and amplitude reference tracking is somehow successful.

4.2.3 Genetic Algorithm's results

Among genetic algorithm results we only have shown the results for case 1 when the total absolute gain value is limited to 60 as it has the best performance. The results for reference tracking are given Figure 4.32 to Figure 4.37.

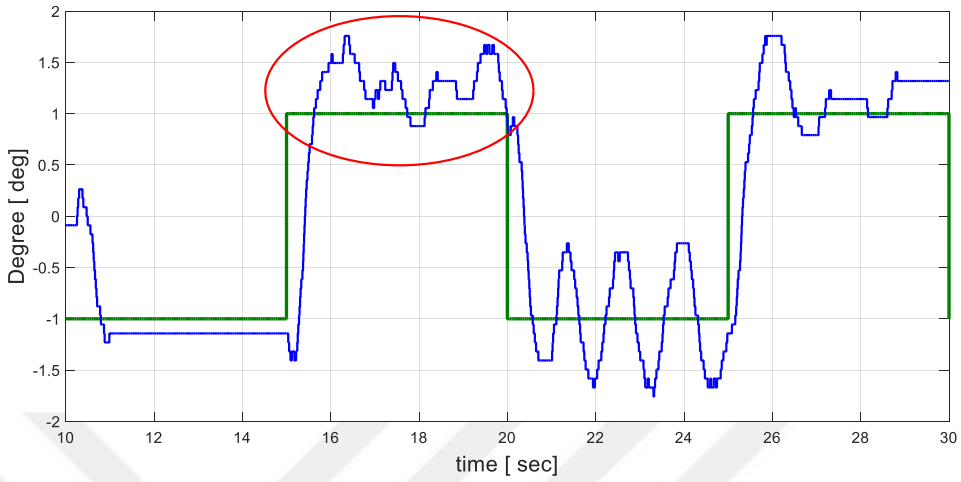

Figure 4.32: *The reference signal in square wave (green) and the arm angle of the system (blue) when f=0.1 Hz for case 1*

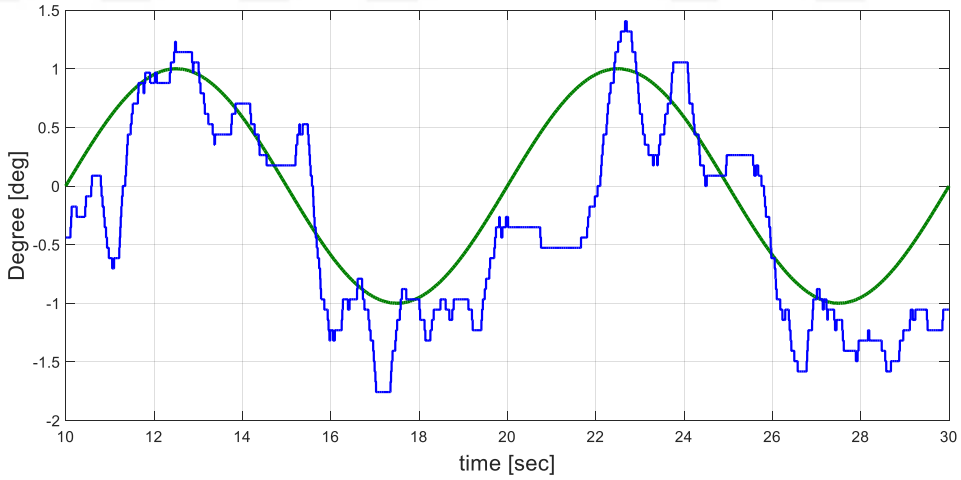

Figure 4.33: *The reference signal in sinusoidal wave (green) and the arm angle of the system (blue) when f=0.1 Hz for case 1*

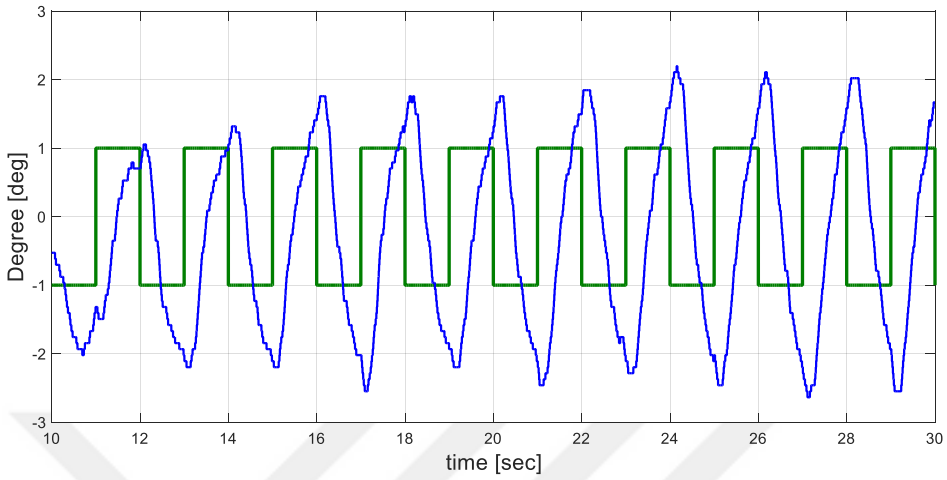

Figure 4.34: *The reference signal in square wave (green) and the arm angle of the system (blue) when f=0.5 Hz for case 1*

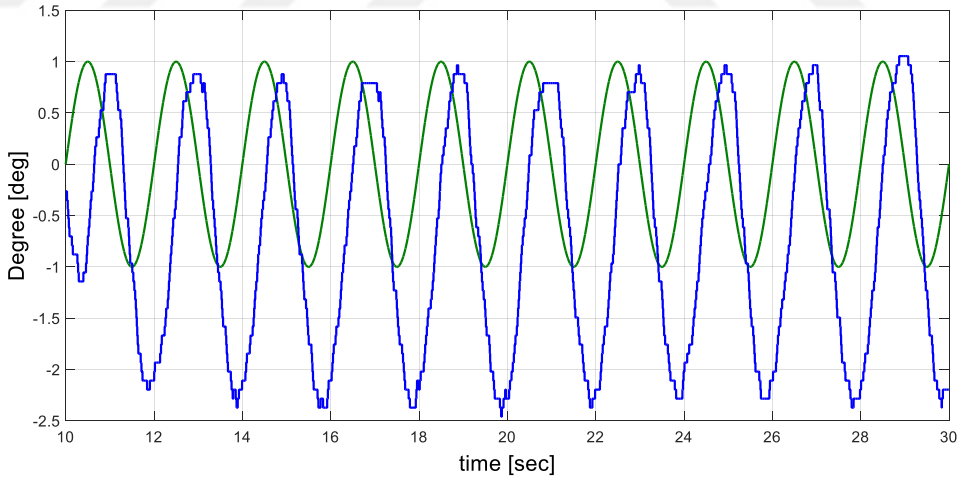

Figure 4.35:*The reference signal in sinusoidal wave (green) and the arm angle of the system (blue) when f=0.5 Hz for case 1*

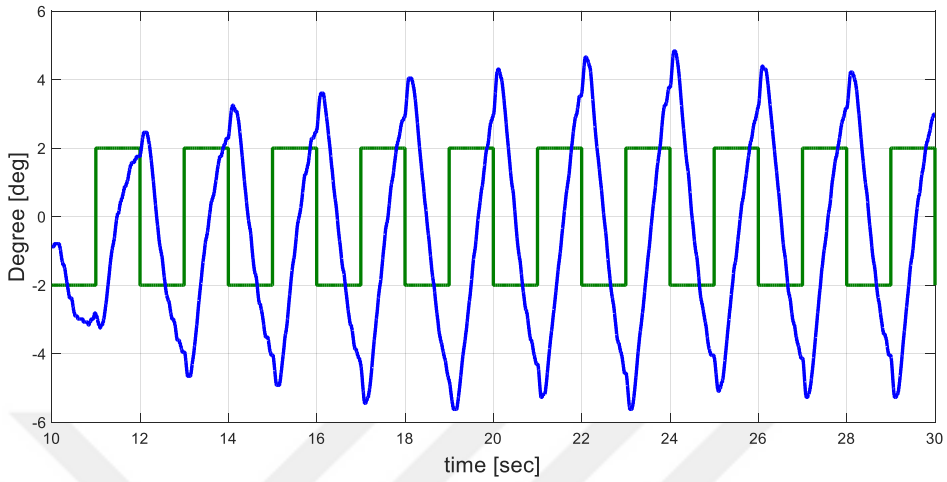

Figure 4.36:*The reference signal in square wave (green) and the arm angle of the system (blue) when f=0.5 Hz amplitude =2 for case 1*

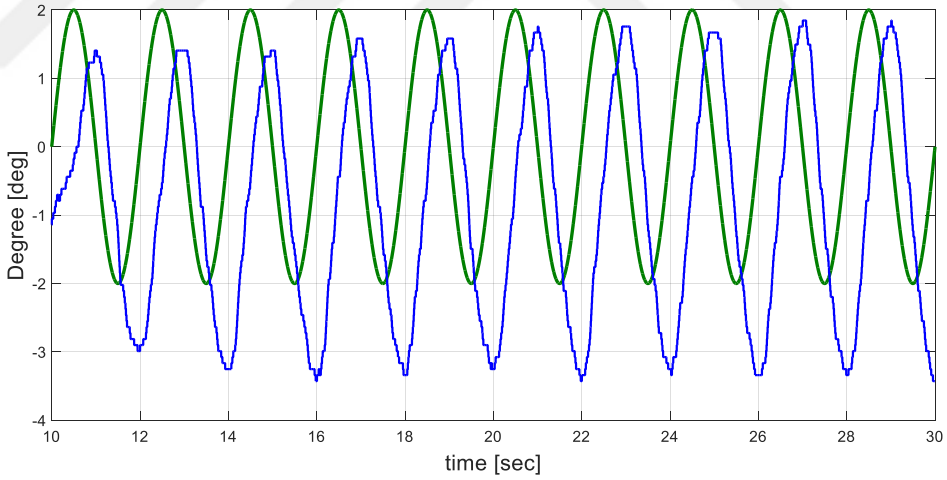

Figure 4.37:*The reference signal in sinusoidal wave (green) and the arm angle of the system (blue) when f=0.5 Hz amplitude=2 for case 1*

In these results generally the controller is successful in tracking reference signals with lower frequencies. However, as the frequency increases the tracking capability decreases still sustaining the pendulum in upright position. Hence we can conclude that the controller is successful in reference signal tracking in general.

4.3 The effects of disturbances

In order to observe effect of disturbances in rotary inverted pendulum, two different extra masses are putting to the arm when the system is stabilized around the equilibrium point. For this purpose, two materials are selected and their masses are 216.2 g and 516.2 g. Then, the arm angle and voltage values are monitored in two conditions: without reference input signal and with reference input tracking condition. In without reference input signal condition, reference input is adjusted as a zero. In other condition, reference input signal is a square wave signal and its frequency 0.1 Hz and its amplitude is 2.

Firstly, real time application is run as in section 4.2, using design controllers, and the position of set point is set to 0. At the 13th second (after the system is stabilized at the unstable equilibrium point), light extra mass (216.2 gram) is put on the rotary arm and the following the arm angle and control voltage signals are observed in. Similar steps are applied for heavy extra mass. To monitor the effects of disturbances, state feedback controller's results and in GA, total value=60 for case 1 are selected.

For the without reference input signal case:

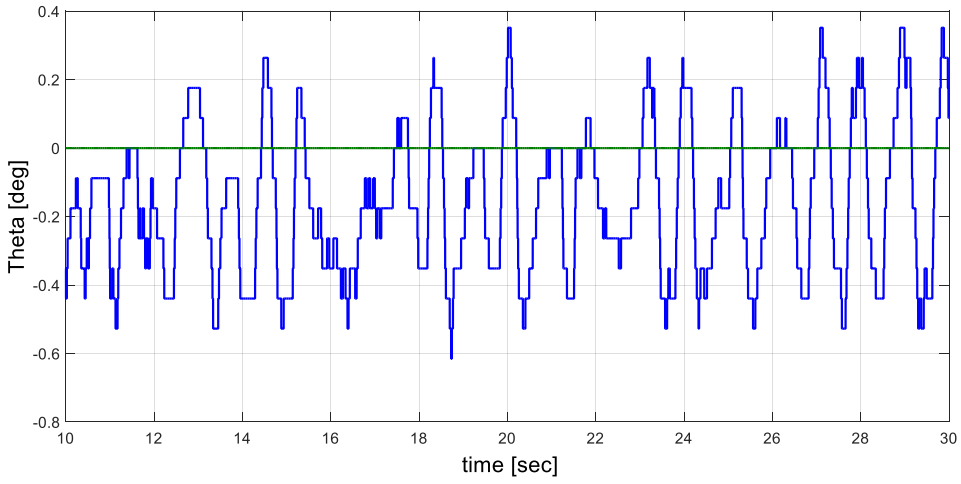

Figure 4.38:*The arm angle in case of a light extra mass disturbance for state feedback controller*

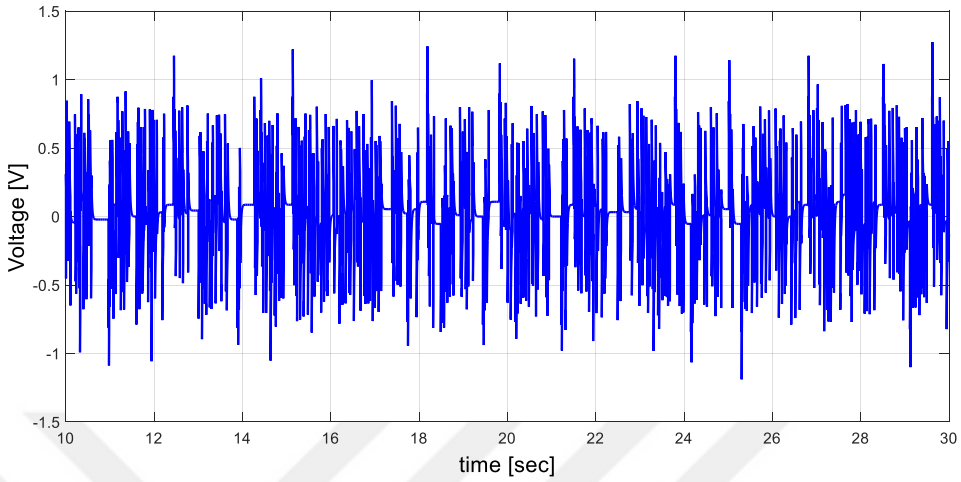

Figure 4.39:*The voltage in case of a light extra mass disturbance for state feedback controller*

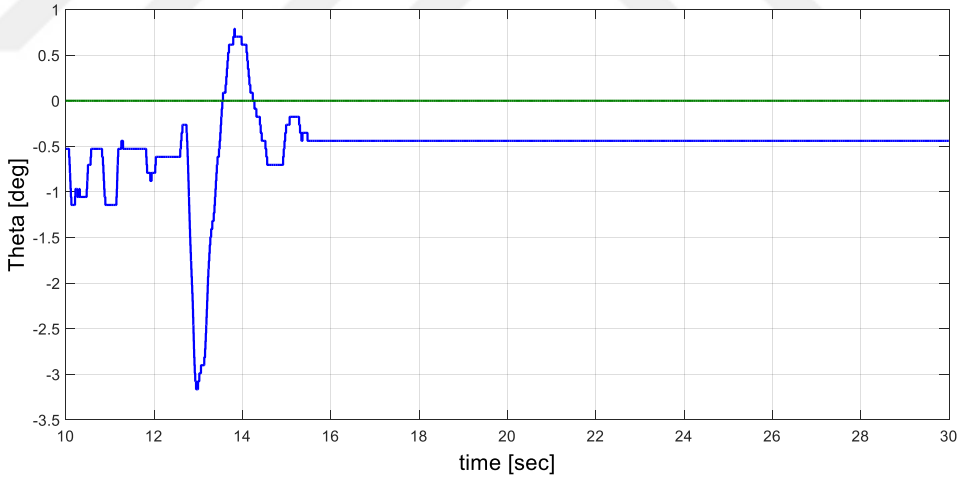

Figure 4.40:*The arm angle in case of a heavy extra mass disturbance for state feedback controller*

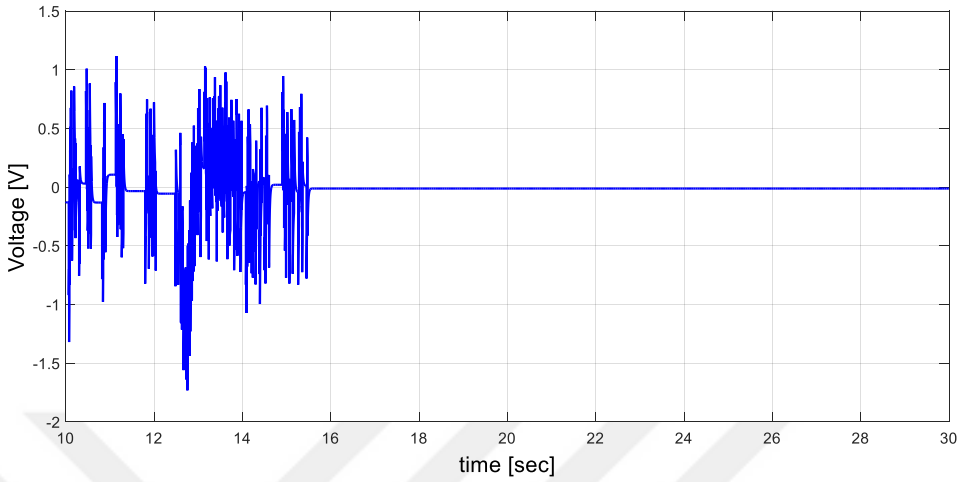

Figure 4.41:*The voltage in case of a heavy extra mass disturbance for state feedback controller*

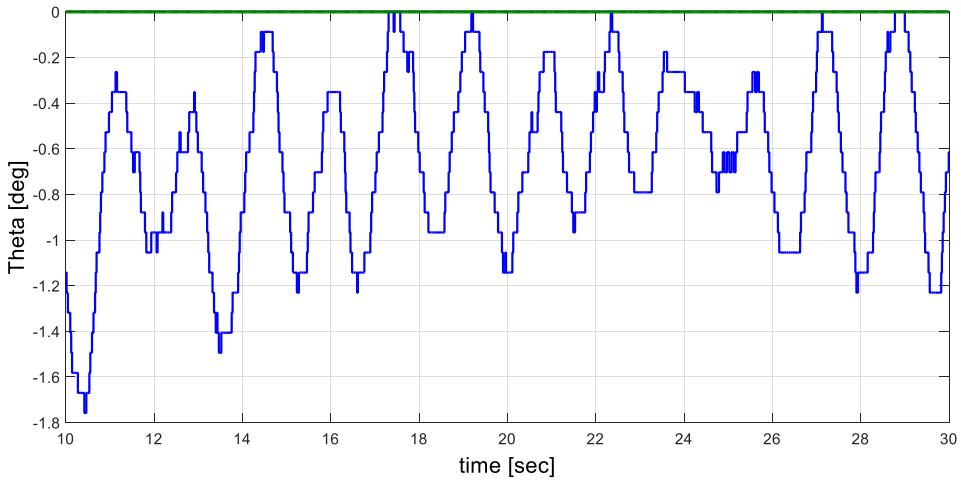

Figure 4.42:*The arm angle in case of light extra mass disturbance for case 1 total gain value=60*

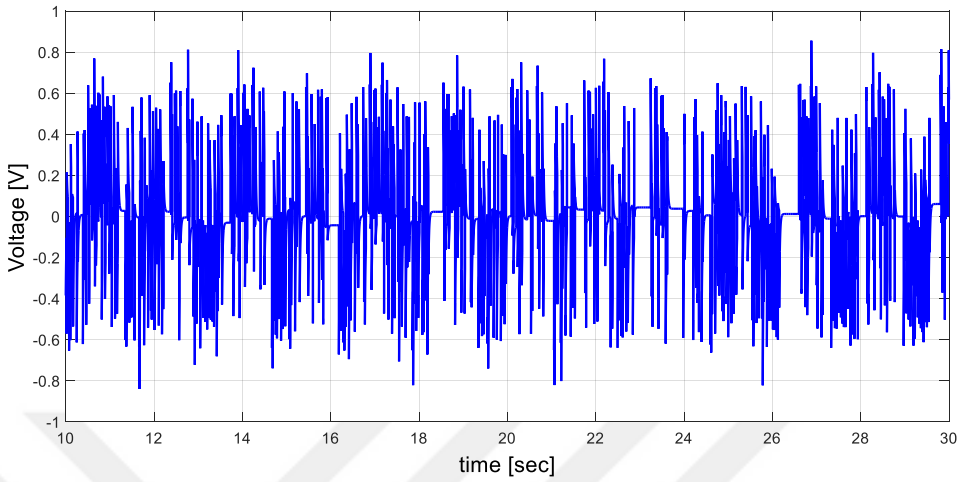

Figure 4.43:*The voltage in case of light extra mass disturbance for case 1 total gain value=60*

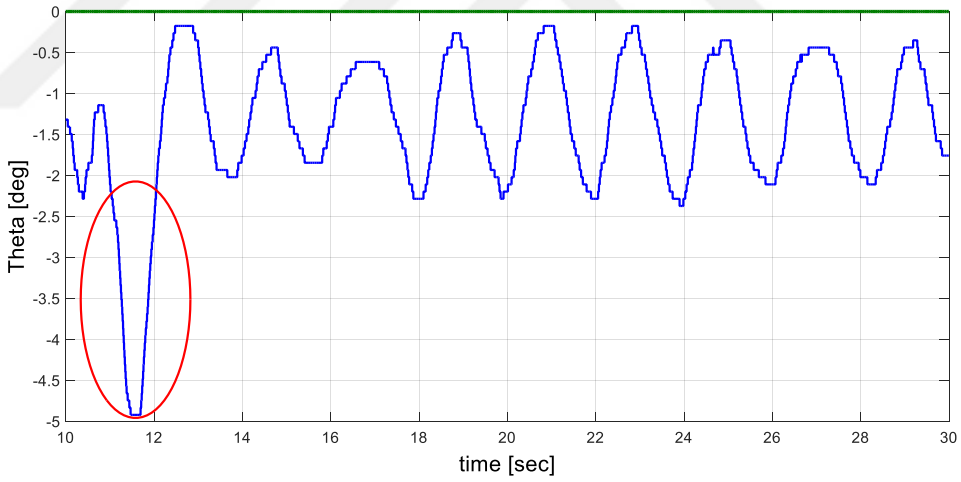

Figure 4.44:*The arm angle in case of heavy extra mass disturbance for case 1*

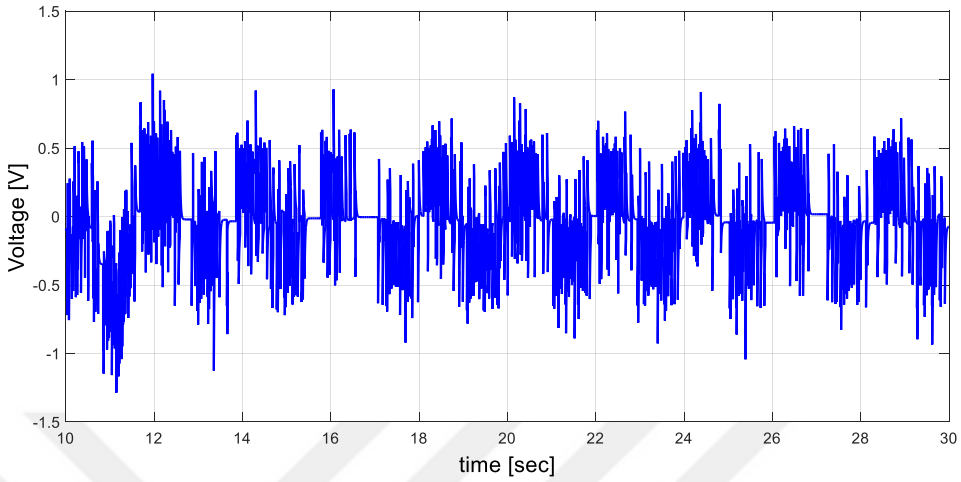

Figure 4.45:*The voltage in case of a heavy extra mass disturbance for case 1 total gain value=60*

For the with the reference input track condition:

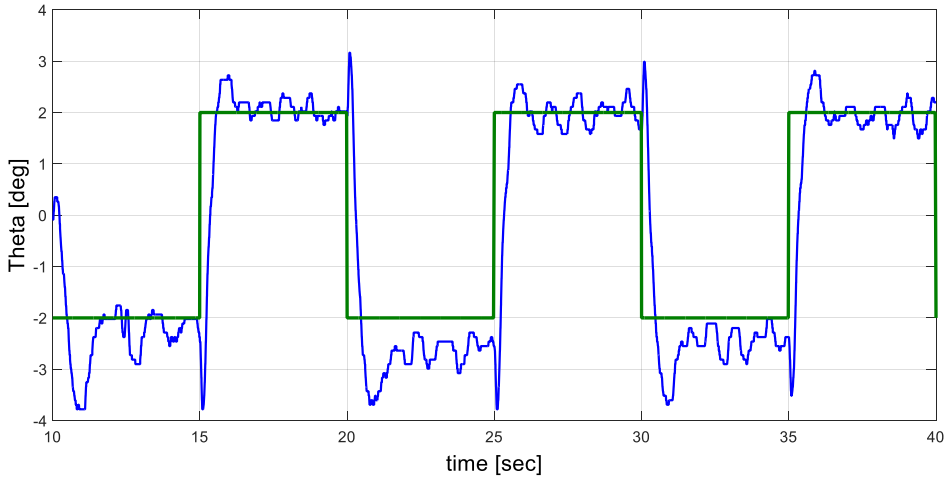

Figure 4.46: *The arm angle (blue) in case of a light extra mass disturbance for state feedback controller and the reference input signal (green)*

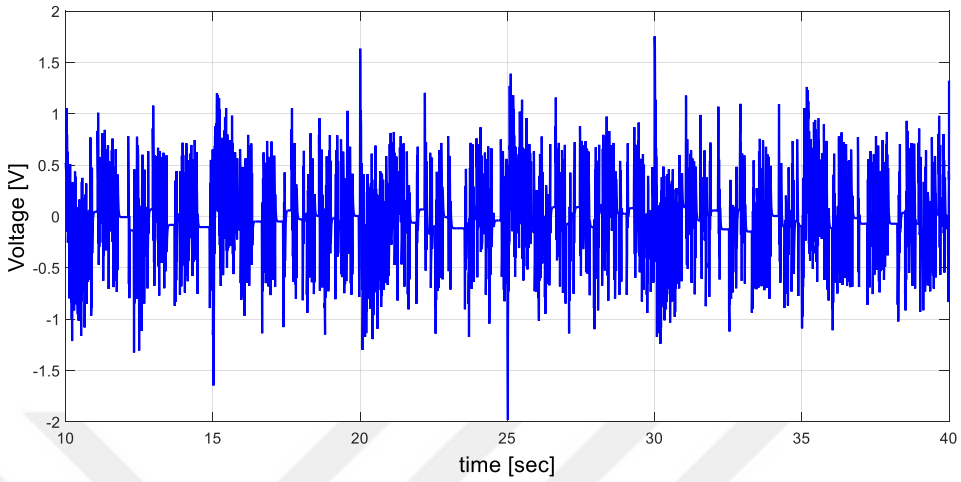

Figure 4.47: *The voltage in case of a light extra mass disturbance for state feedback controller in the reference input signal tracking condition*

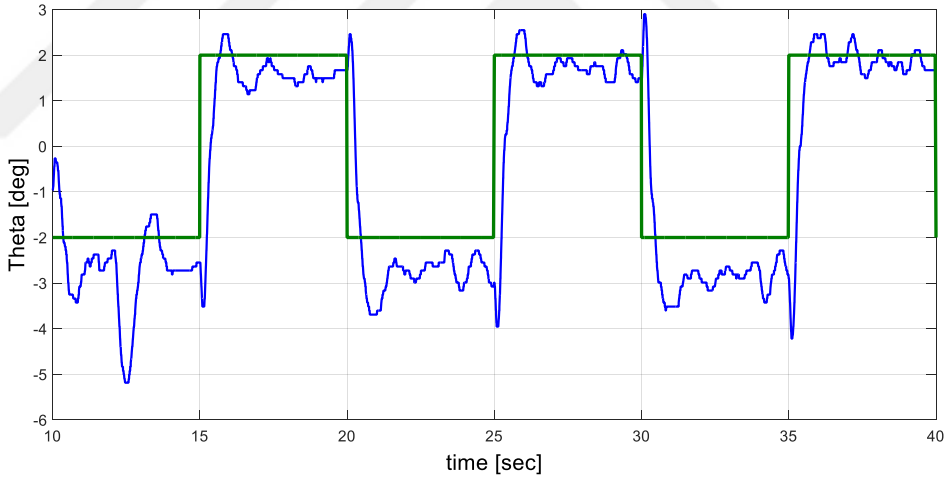

Figure 4.48:*The arm angle (blue) in case of a heavy extra mass disturbance for state feedback controller and the reference input signal (green)*

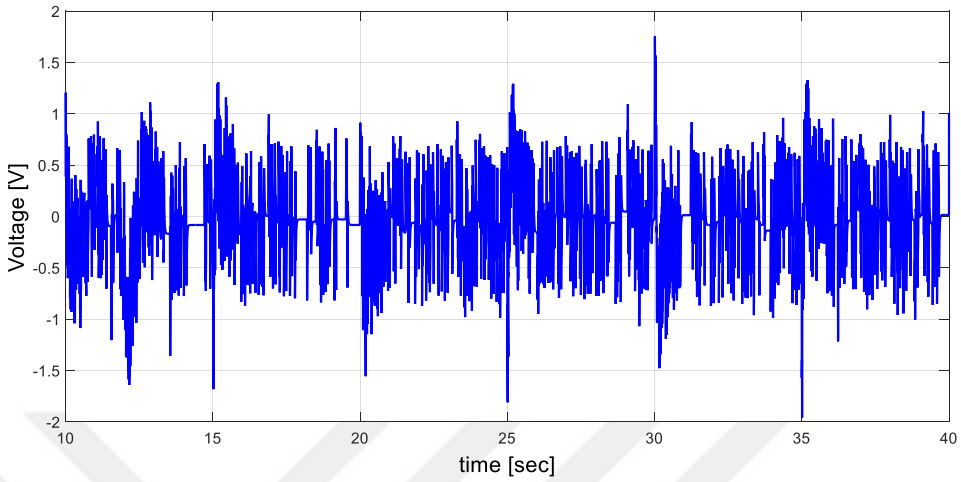

Figure 4.49: *The voltage in case of a heavy extra mass disturbance for state feedback controller in the reference input signal tracking condition*

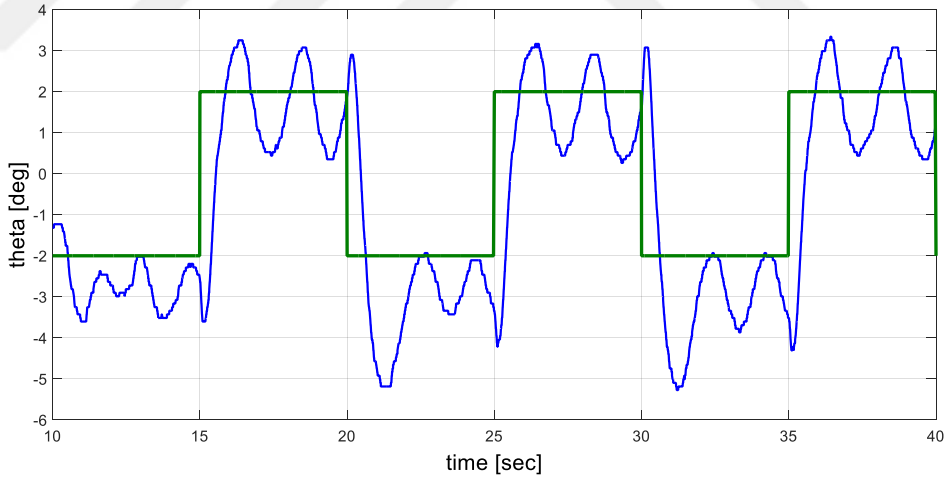

Figure 4.50:*The arm angle (blue) in case of a light extra mass disturbance for case 1 total gain value=60 and the reference input signal (green)*

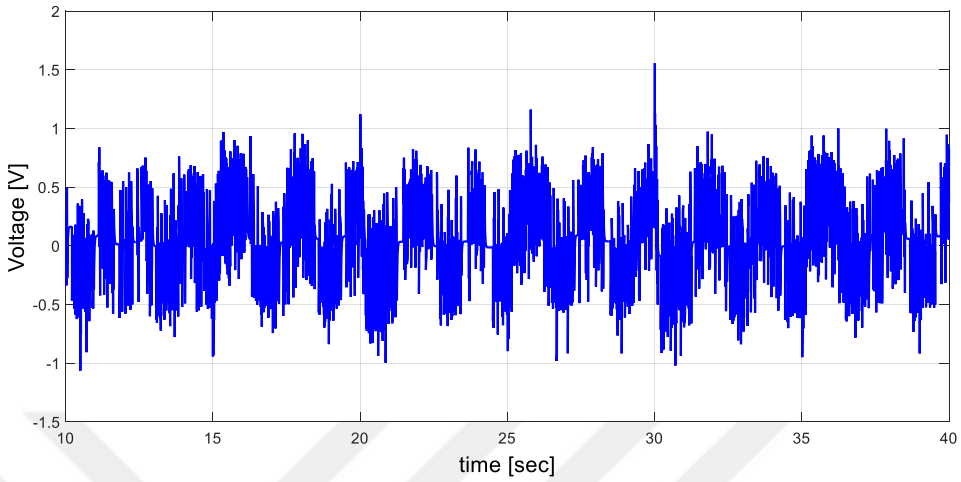

Figure 4.51:*The voltage in case of a light extra mass disturbance for case 1 total gain value=60 in the reference input signal tracking condition*

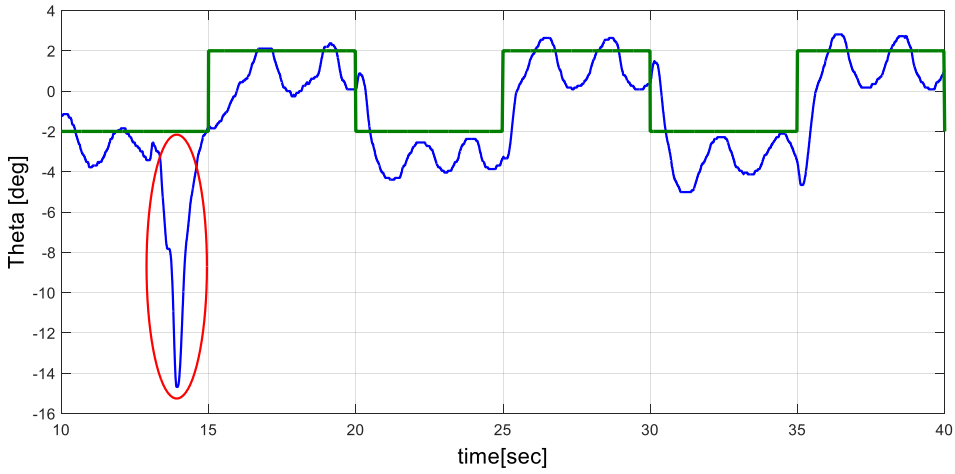

Figure 4.52:*The arm angle (blue) in case of a heavy extra mass disturbance for case 1 total gain value=60 and the reference input signal (green)*

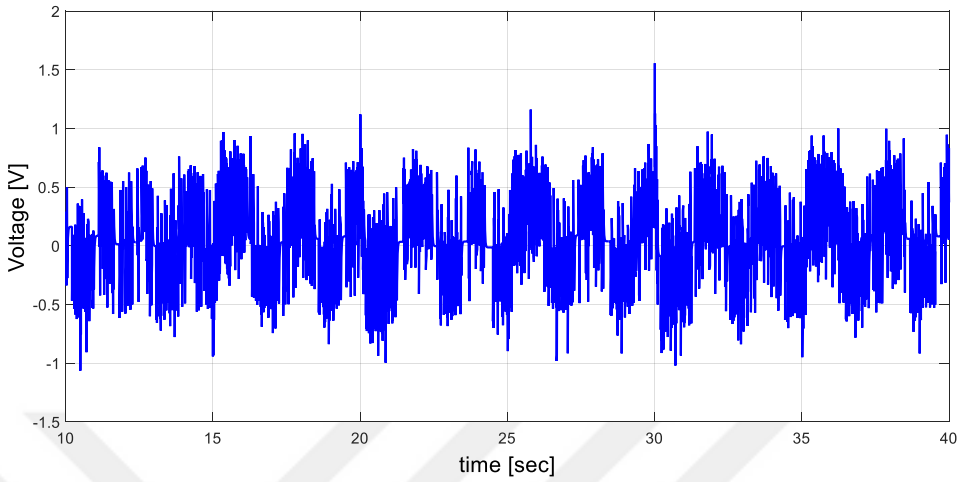

Figure 4.53: *The voltage in case of a light extra mass disturbance for case 1 total gain value=60 in the reference input signal tracking condition*

In all disturbance conditions both the state feedback controller with lower DC motor efficiency values and the controller obtained by genetic algorithm shows satisfactory results. According to the Figure 4.44 and Figure 4.52, when the disturbance is added, the difference between reference input and the arm angle is high. After this time, the arm angle tracks the reference input.

4.4 Performance index measurement of controller

In control theory, a performance index is a quantitative measurement of the performance of the system. This index is chosen to meet design specifications of important parameters of the system. An optimum control system is that the system parameters are arranged so that the index reaches an extremum value, commonly a minimum value. There are some common performance indexes such as:

- Integral Square Error (ISE)

$$ISE = \int_{t=0}^{t=\infty} e^2(t)dt \tag{4.1}$$

- Integral of Absolute Magnitude of Error (IAE)

$$IAE = \int_{t=0}^{t=\infty} |e(t)|dt \tag{4.2}$$

- Integral Time Absolute Error (ITAE)

$$ITAE = \int_{t=0}^{t=\infty} t|e(t)|dt \tag{4.3}$$

- Integral Time Square Error (ITSE)

$$ITSE = \int_{t=0}^{t=\infty} te^2(t)dt \tag{4.4}$$

In all of the above equations e(t) represents error response of the system. Integral defines between 0 and ∞. But, upper and lower limits can be changed depending on system response duration.

In this thesis, integral square error for the arm angle and power of the applied input signal (voltage) are defined as the performance index values. As the system signals are (arm angle and applied voltage) have discrete nature instead of exact computation an approximation is used. In the integral square error computation (the same is valid for power calculation), the upper and lower limits of integration are chosen as 15 and 25 seconds of real time applications (as signals seem to be in steady state condition in this duration).

The sampling rate of the data is 1000 Hz between these two limit values hence there are 10000 data available. So, between each consecutive data there is a time step of 0.001 seconds. Then the approximation for the integral square error for arm angle equation becomes;

$$\sum_{i=1}^{10000} (\theta_i - 0)^2 \times 0.001 \tag{4.5}$$

For the input voltage signal, the power can be written as

$$\sum_{i=1}^{i=10000} Voltage_i{}^2 \times 0.001 \tag{4.6}$$

For comparison, default setup, state feedback controller with efficiency and in genetic algorithm case 1 and case 3 when the total absolute gain value is limited to 60 cases are selected and the results are tabulated.

Table 4.5: *The results of performance of measurement controller*

Case	ISE for arm Angle	Power of Voltage Signal
Default (Setup)	119.7017	0.7657
State Feedback Controller (with efficiency)	1.7146	0.8070
Case 1 total absolute gain value is limited to 60	2.1810	0.5166
Case 4 total absolute gain value is limited to 60	3.8257	2.1044

Default (setup) case is the worst case among other cases as it has a high ISE value. In genetic algorithm cases, especially case 1 power of the applied voltage signal is the least one hence it can be concluded that the controller balances the system by relatively a small effort with respect to other controllers as its ISE value for the arm angle is also relatively small. The state feedback controller is also a good choice as it has the best ISE value with slightly higher voltage signal power value.

CHAPTER 5

CONCLUSIONS AND RESULTS

In this thesis, main purpose is to obtain state feedback controllers by genetic algorithm due to optimization of a multi-criteria cost functions. These controllers are designed for highly nonlinear, complex and unstable system. In order to complete the design some procedures are accomplished in an order one by one. Initially, using dynamics of the system, the nonlinear equations of the system are determined. These equations are linearized around the unstable equilibrium point. From linear equations, the information about of this system such as state space matrices, eigenvalues are determined. In the lights of these information, the system is stabilize using state feedback controllers. While obtaining state feedback controller by genetic algorithm different cost criteria are set. These criteria include the general stability criteria of the linearized system (Routh Hurwitz table) and relative stability criteria that corresponds to replacing closed loop eigenvalues of the system to suitable locations (they should be to the left of s= -2, their imaginary part/real part ratio should be smaller than a threshold value) and criteria related with state feedback gain values. Hence in total genetic algorithm optimization runs turns into a multi criteria optimization method to produce state feedback controllers. In the real time applications, the produced controllers as the result of optimization process are tested. For each real time run, the arm angle, the pendulum angle and applied voltage waveforms are observed and variables are compared for all cases.

The designed controllers by genetic algorithm are more successful than set-up controller. In both methods, eigenvalues are non-positive. Hence, the system is stable for all cases.

In reference signal tracking and application of disturbance the sate feedback controller (obtained for less DC motor efficiency) and the seemingly best controller obtained by

genetic algorithm are compared. The controller obtained by genetic algorithm has given better results in reference signal tracking in general. In the presence of mass type of disturbances, the controllers generally demonstrated similar performances.

In the future works, a deeper analysis should be carried out in order to identify the effects of swing up mode parameters and gain values of state feedback controller in stability and transient and steady state responses.

REFERENCES

[1] B. Prakash, B. K. Roy, and R. K. Biswas, "Design, implementation and comparison of different controllers for a rotary Inverted Pendulum," *1st IEEE Int. Conf. Power Electron. Intell. Control Energy Syst. ICPEICES 2016*, pp. 1–6, 2017.

[2] K. Nath and L. Dewan, "Control of a rotary inverted pendulum via adaptive techniques," *2017 Int. Conf. Emerg. Trends Comput. Commun. Technol. ICETCCT 2017*, vol. 2018-January, pp. 1–6, 2018.

[3] E. Duart, J.L.; Montero B.;Ospina, P.A.; González, "Dynamic Modeling and Simulation of a Rotational Inverted Pendulum," *J. Phys. Conf. Ser.*, vol. 755, no. 1, 2016.

[4] K. Furuta, M. Yamakita, and S. Kobayashi, "Swing-up Control of Inverted Pendulum Using Pseudo-State Feedback," *Proc. Inst. Mech. Eng. Part I J. Syst. Control Eng.*, 2007.

[5] R. L. Haupt and S. E. Haupt, *"Practical genetic algorithms."* New York: John Wiley &Song, inc. publication, 2004.

[6] D. E. Goldberg, *David E. Goldberg-Genetic Algorithms in Search, Optimization, and Machine Learning-Addison-Wesley Professional (1989).pdf*. 1989.

[7] I. Kolcu, "An Investigation Of Genetic Algorithms And Genetic Programming," 1996.

[8] R. H. Dorf, Richard C. Bishop, *Modern Control Systems*, 12th ed. Prentice Hall, 2010.

[9] "Quanser Inc. Rotary Inverted Pendulum Workbook," 2011.

[10] "Quanser Inc. Rotary Inverted Pendulum User Manual," *SpringerReference*, 2011.

[11] A. Al-jodah and H. Zargarzadeh, “Experimental Verification and Comparison of Different Stabilizing,” 2013.

[12] “SRV02 ,USER MANUAL,” 2008.

[13] “GA Roulette wheel selection.” [Online]. Available: http://www.edc.ncl.ac.uk/highlight/rhjanuary2007g02.php. [Accessed: 13-Jun-2019].